International Journal of Environmental Science and Technology
https://doi.org/10.1007/s13762-021-03256-8

REVIEW

A comprehensive review on the role of some important nanocomposites for antimicrobial and wastewater applications

T. Naseem[1] · **M. Waseem**[2]

Received: 9 November 2020 / Revised: 8 February 2021 / Accepted: 6 March 2021

Abstract

Water is crucial for the existence of life. The world, however, is facing a global water crisis. There are variety of microorganisms, gases and other toxins responsible for water contamination. Various types of nanomaterials exist that have enormous potential to treat contaminated water (water containing metal toxins or specific organic or inorganic impurities) due to their unique properties such as a high surface area and their ability to work effectively even at low concentrations. In recent years, scientists have been giving considerable attention to the application of nanocomposites for water purification, wastewater treatment, microorganism elimination, chemical contaminants, heavy metals removal and so forth. The incorporation of different nanofillers such as carbon nanotubes, graphene oxide, 2D materials, zinc oxide, titanium dioxide, copper and silver nanoparticles into polymeric materials has facilitated important advances, such as suppressing the accumulation of pollutants and foulants, improving the hydrophilicity, increasing the efficiency and improving the mechanical properties. This review discusses leading advances in the development of nanocomposites for antimicrobial and wastewater treatment with the aim of providing an improved understanding of nanocomposites and their applications in antimicrobial and wastewater treatment. Nanocomposites incorporating nanoparticles and graphene or its derivatives are frequently used in the treatment of wastewater and antimicrobial activities. Nanocomposites loaded with silver (Ag) nanoparticles are highly effective for wastewater treatment and have powerful antimicrobial activities. Nanostructured catalytic membranes and nano-photocatalysts are efficient and eco-friendly tools for the removal of contaminants from wastewater and antimicrobial activities, but they require more research and investment.

Keywords Adsorption · Antibacterial activity · Nanocomposite · Photocatalytic degradation · Wastewater treatment · Nanoparticles

Introduction

Water is a basic requirement for human life. However, we are far from meeting global requirements for clean water, and this issue will continue to grow over the time (Hillie and Hlophe 2007; Elwakeel et al. 2020b). The demand of clean drinking water is rising as a result of the deterioration of water quality, global climate change and population growth (Tchobanoglous et al. 1991; Elwakeel et al. 2020d). Emissions of organic dyes and heavy metal ions from the paper, leather and textile industries are a serious problem, as they are potentially mutagenic and carcinogenic. To meet environmental requirements, wastewater contaminated with these organic and inorganic species need to be treated before being discharged (Santhosh et al. 2016; Elwakeel et al. 2021). Heavy metals are widely used in various industries for many purposes, including mining and pigment production. Synthetic dyes are also an important type of pollutant, and their sources for water contamination include the textile, pulp and paper, tinting, printing, painting and tanning industries. The removal of dye from such wastewater is a challenging task, as pigments and synthetic dyes are biodegradation-resistant and remain in the environment for a long time. The destruction and handling of organic dyes is therefore an important issue, and a cost-effective method for

Editorial responsibility: J Aravind.

✉ M. Waseem
waseem_atd@yahoo.com

[1] Department of Chemistry, University of Azad Jammu and Kashmir, Muzaffarabad 13100, Pakistan

[2] Department of Chemistry, COMSATS University Islamabad, Islamabad, Pakistan

Published online: 04 April 2021

removing dye substances from wastewater has been developed (Santhosh et al. 2016; Elwakeel et al. 2018).

Water impurities can be biological, organic or inorganic. Some contaminants are harmful, carcinogenic and toxic to humans and ecosystems, and some heavy metals have very toxic impurities (El-Liethy et al. 2018). Since ancient times, arsenic has been known to be a fatal element. Chromium, cadmium, copper, mercury, zinc, lead, nickel and others are also highly toxic heavy metals that can have serious toxic effects (Elwakeel et al. 2020a). Furthermore, the following nitrates have a high-level hazardous effect: fluorides, phosphates, selenides, chlorides and chromates. Toxicity is also associated with organic pollutants such as detergents, fertilizers, phenols, hydrocarbons, pesticides, biphenyls, oils and fats. Pharmaceuticals and personal care products (PPCPs) are generally resistant to natural biodegradation. The PPCP concentration in water varies from mg/L to µg/L. Conventional water treatment results have been largely unsatisfactory, as treatment plants are not prepared to remove persistent low-sulphur impurities.

Efficient and environmentally friendly methods of eliminating such pollutants are important (de Mendonça et al. 2019; Elwakeel et al. 2020c). For wastewater treatment, various strategies are used such as solvent extraction, evaporation, ultrafiltration and reverse osmosis. However, these methods extract water impurities without creating harmful end products (Anjaneyulu et al. 2018). To reduce the effects of contaminants, the goal of each oxidative process is to produce and use a hydroxyl free radical (HO) as a powerful oxidant. After activation, hydrogen peroxide may be used as an oxidant such as UV radiation (Slokar and Marechal 1998), as a metal ion or a Fenton's reagent. Different approaches for removing metal ions and dyes including photocatalysis, adsorption, electrochemical precipitation and reverse osmosis are discussed in the literature (Fan et al. 2016; Santhosh et al. 2016; Ezzatahmadi et al. 2017). However, among these methods, only adsorption is inexpensive, fast and commonly applied. Photocatalytic degradation processes are also an attractive option, as they use radiant energy to promote the desired degradation. Some examples of photocatalytic degradation processes are peptide dye breakdown (Robinson et al. 2001; Petica et al. 2017) and self-cleaning (Anandan et al. 2013) applications.

In recent years, environmental cleanup applications have become an active area of heterogeneous photocatalysis. To reduce the organic pollutants in water, harmless semiconductor materials are mainly used. Zinc oxide and titanium oxide have been used for the photocatalytic degradation of textile coating wastewater under ultraviolet radiation. When titanium dioxide was used at 303 K, the maximum color removal rate reached 96% after 2.5 h of irradiation, whereas when zinc oxide was used at the same temperature and time, an 82% color reduction was observed (Attia et al. 2007). Pairs et al. used the artificial photocatalytic degradation of lysine fast yellow dye using a zinc oxide suspension (Pare et al. 2009). Azo dye orange II has been tested for photocatalytic decoloration in water in an external UV-irradiated suspension of zinc oxide (ZnO) (Nishio et al. 2006).

Due to nanocomposites' special properties, such as high strength, high rigidity, high durability, low density, high resistance, corrosion resistance, gas barrier and heat resistance, they provide many advantages over other materials. Nanocomposites are multi-phase materials in which a minimum of one of the phases displays sizes in the range of 10–100 nm (Sharma et al. 2019). Nanocomposites are widely used in various areas including life sciences, the distribution of pharmaceuticals and the treatment of wastewater. In nanocomposites, nanoparticles are fused into a range of usable materials such as a CNT multi-wall, activated carbon, low-cost graphene oxide and polymeric media. Nanocomposites are used in a variety of fields such as food packaging, protection against anticorrosion, biomedical applications and coating (Veprek and Veprek-Heijman 2008; Azeredo 2009; Rhim et al. 2013; Sharma et al. 2019).

This paper presents a detailed review of nanocomposites and their wastewater treatment. Figure 1 shows the block diagram of the nanocomposites that are discussed in detail

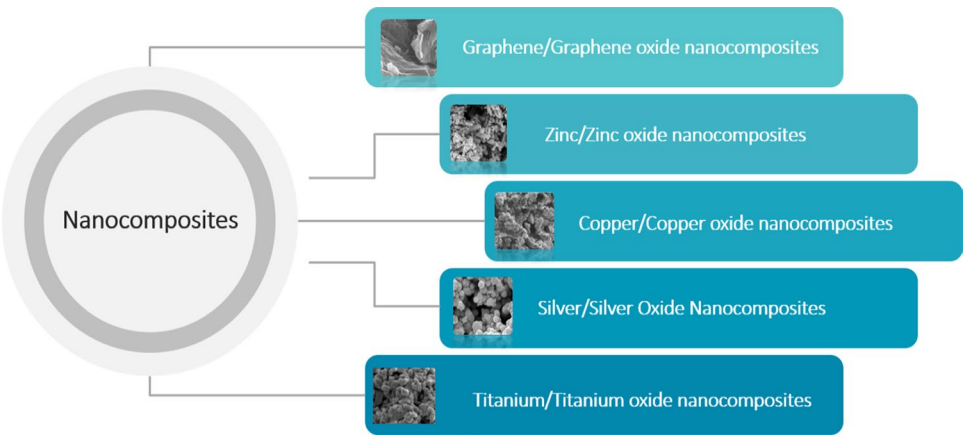

Fig. 1 Nanocomposites for water purification

in this paper. To the best of the authors' knowledge, in the literature, no review paper exists that discusses nanocomposites in detail for water purification.

Wastewater in area of focus

Wastewater is a type of waste liquid product produced by industrial, agricultural and municipal activities. This waste liquid contains pollutants such as organic materials, microorganisms, toxic heavy metals and soluble inorganic compounds. These pollutants modify the biological, chemical and physical characteristics of clean water (Abou El-Nour et al. 2010). They can be classified according to the waste sources into municipal and industrial wastewater. Municipal waste sources are from homes and commercial activities, and this wastewater often contains faeces and urine. Sources of industrial wastewater are the industrial and agricultural activities, and this wastewater, in addition to domestic compositions, also contains organic and inorganic chemicals (Adams et al. 2006). Wastewater contains high micro-organism concentrations, including protozoa, bacteria, viruses and toxic chemicals such as heavy metals, trace elements and radionuclides.

Therefore, wastewater is one of the most important sources of waterborne diseases, some of which are fatal such as typhoid and cholera. In 2004, polluted water caused the deaths of nearly 1.6 million children under five years old (AL-Thabaiti et al. 2008; Baek and An 2011). Figure 2 shows different types of pollutants that can be found in water. To protect the environment from pollution, wastewater treatment must be considered as an area of personal and governmental-level investigation. Physical, chemical and biological processes may be involved in cleaning up water from different contaminants (Borgohain and Mahamuni 2002; Bitton 2005).

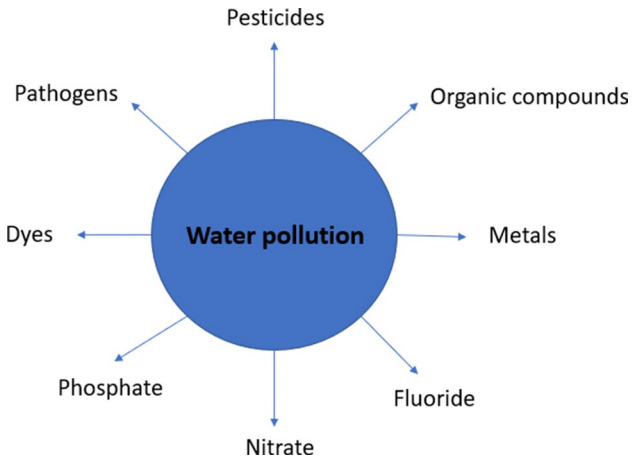

Fig. 2 Different possible pollutants in water

Wastewater characteristics

Wastewater characteristics can be classified into biological, chemical and physical characteristics.

Physical characteristics

Wastewater possesses numerous physical characteristics, such as total solids, dyes and others (volatile, fixed, suspended and dissolved) (Borgohain and Mahamuni 2002). The total dissolved solids (TDS) are, however, dissolved matters in wastewater and may include inorganic salts and metals such as magnesium, chlorides, bicarbonates, calcium, sodium and potassium, including small amounts of organic materials. The sizes of these particles range from 0.01 to 1.00 µm for dissolved solids (Cheremisinoff 2002; Chowdhury et al. 2011). According to the United States Environmental Protection Agency, the maximum contaminant level (MCL) of TDS in drinking water must be less than 500 ppm, because high levels of TDS can cause many effects such as dry skin and a poor taste (Chowdhury et al. 2011). Total suspended solids (TSS) are the suspended inorganic and organic materials in wastewater. TSS were retained in a 1.2-µm-pore-size filter when wastewater was filtered, while dissolved solids passed through the same filter (Cioffi et al. 2005).

Chemical characteristics

Wastewater chemical pollutants can be classified as organic, inorganic and gaseous chemicals (Naseem and Durrani 2021).

Organic pollutants

Many organic impurities are present in wastewater. Generally, these are carbohydrates, proteins, oils and fats at about 50%, 40% and 10%. The primary organic pollutants of wastewater are impurities and surfactants (Adams et al. 2006). The chemical demand for oxygen (COD) and biological demand for oxygen (BOD) are two functional measures of organic water pollution quality. BOD is defined as the dissolved oxygen in wastewater required for aerobic microorganisms that decompose organic contaminants and is therefore used as a parameter for determining organic matter concentrations in wastewater. The most commonly used test is BOD5, which measures the BOD of effluent for five days at 20 °C (Adams et al. 2006).

Inorganic pollutants

Wastewater contains several inorganic pollutants such as heavy metals, trace elements of phosphorus, nitrogen compounds and other inorganic ingredients. Toxic inorganic metals such as lead (Pb), barium (Ba), arsenic (As), cadmium (Cd), mercury (Hg) and others may exist in drinking water in limited quantities, depending on their health effects.

The presence of cadmium should be less than 1 µg/L in food or water; otherwise, it can have impacts on both the health of humans and animals such as high blood pressure, liver disease, painful osteomalacia and brain and kidney damage (Mousa 2013). The main sources of lead in water are manufacturers, mining, plumbing and the deposition of gasoline exhaust (Mousa 2013). Levels of lead higher than 0.015 mg/L in water cause some health effects such as central and peripheral nervous system effects and kidney damage (Ellis 2004). Mercury is used in many applications such as in thermometers, antiseptics, batteries and dental amalgams. It can be found in water in the form of organometallic compounds (such as alkylmercurials), inorganic compounds (such as $HgCl_2$) and elemental mercury. There are many health effects of mercury such as kidney damage; therefore, the MCL for Hg in drinking water is very low at about 0.002 mg/L (Evangelou 1998).

Water quality can be affected by other inorganic pollutants such as pH, free and total chlorine, sulphate, phosphorus, sodium and nitrogen. However, the optimum pH for drinking water should be less than 8. Also, to maintain the drinking water's quality, the concentrations of sodium and sulphate should be less than 200 and 250 mg/L, respectively. However, the presence of sulphate at high concentrations can cause noticeable taste and laxative effects, while concentrations of chlorine higher than 5 mg/L can cause a bad taste or smell in water (Chang and Zeng 2004).

Biological characteristics

Biological characteristics are present in addition to the chemical and physical characteristics of wastewater, and the biological contaminants in wastewater are living pathogens. Bacteria, viruses and protozoa that can lead to acute and chronic health effects are the main wastewater microorganisms. Bacteria are prokaryotic with different shapes such as spheres, rods and spirals for *Streptococcus aureus*, *Bacillus subtilis* and *Vibrio cholera*, respectively (Fu et al. 2005). The size of bacteria can vary according to their type and shape, but in general their size ranges from 0.1 to 2 µm (Fuqua 2010). Various types of bacteria may be responsible for various diseases in the water supply, such as cholera, typhoid and shigella. However, in wastewater with less serious manifestations, many types of bacteria may exist such as *Enterobacter*, *Escherichia coli*, *Streptococcus faecalis* and *Klebsiella pneumonae*.

Nanotechnology in water purification

Various treatment technologies exist for removing wastewater pollutants such as coagulation, membrane processes, electrochemical oxidation/degradation, photocatalytic oxidation/degradation, photo-Fenton treatment, adsorption, sedimentation, biological oxidation, AOPs, flocculation, oxidation with chemical oxidants and combined methods. Figure 3 shows the different methods used for the purification of water.

For wastewater treatment, nanotechnology offers innovative solutions for adsorption, catalysis, sensors and optical electronics with a high reactivity and adjustable pore volume; high aspect ratio; and electrostatic, hydrophobic and hydrophilic interactions (Daus et al. 2004). Nanotechnology-based processes offer versatile, high performance and cheap water and wastewater solutions. Nanotechnology-based materials represent a major challenge to existing materials and hence could be economically expanded to restore and clean unusual water sources.

Industrial waste treatment with nanomaterials/nanocomposites is also important and extensively used. Figure 4 shows applications of nanocomposites in wastewater treatment. In wastewater treatment, nanotechnology is beneficial because it removes impurities and helps obtain purified water, which leads to a reduction in labour, time and cost (Qu et al. 2013).

Nanomaterials are typically less than 100 nm and contain materials with new biological, physical and chemical properties that are significantly altered (Theron et al. 2010). The properties of nanomaterials, such as high surface adsorption and high photocatalytic reactivity, offer good disinfectant and biofouling antimicrobial properties. The key drawbacks of traditional water purification methods are illustrated in Table 1.

Nano-adsorption

Adsorption usually occurs through physical forces, but sometimes it occurs due to poor chemical bonds (Faust and Aly 1983). Due to its surface area and a lack of selectivity, the effectiveness of conventional adsorbents can be limited (Qu et al. 2013). Nano-adsorbents are typically used for water and wastewater inorganic and organic impurities. They are ideal adsorbents because of their exceptional properties such as their catalytic potential, small size, high surface area, high reactivity, easy separation or the active locations of many different contaminants (Ali 2012).

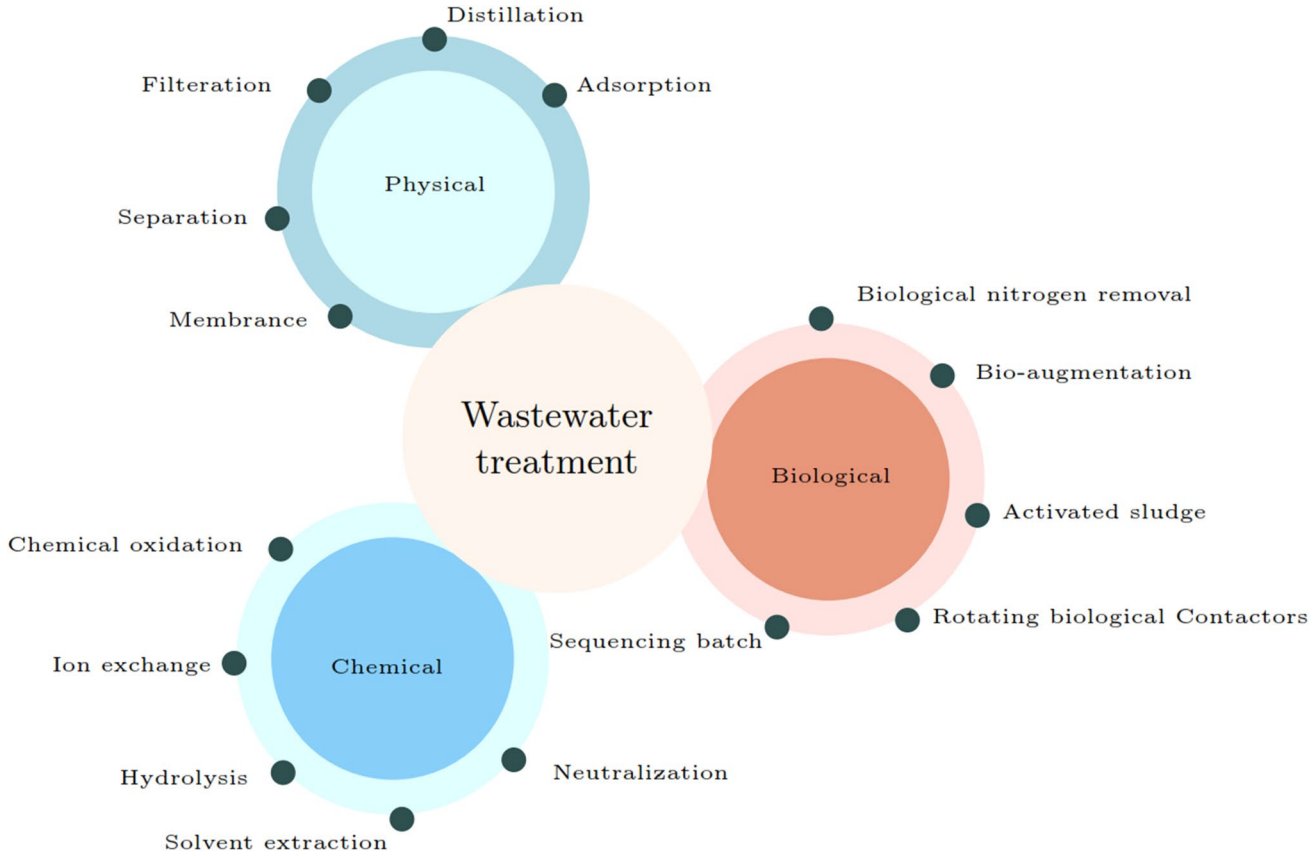

Fig. 3 Different methods used in the treatment of wastewater

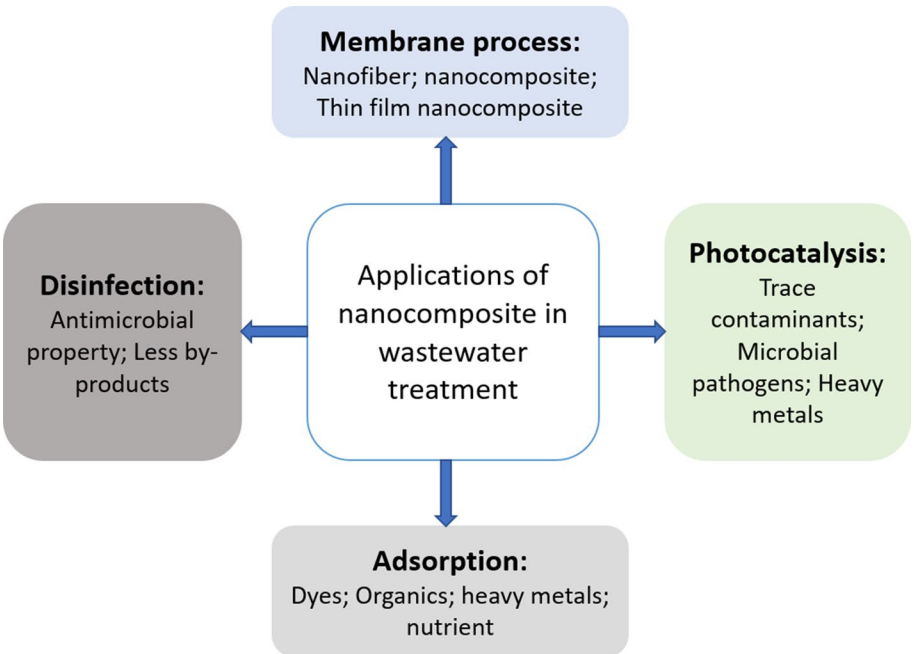

Fig. 4 Applications of nanocomposites in wastewater treatment

Table 1 Limitations of conventional water purification methods

Conventional method	Limitations
Distillation	The majority of pollutants are left behind, and a lot of energy and water are required. Contaminants that have a boiling point > 10 °C are difficult to remove
Chemical transformation	Excess reagent is necessary for chemical transformation. The substance can be a mixture of low quality and cannot be released into the environment and cannot be used in certain difficult conditions. This approach is not very accurate
Coagulation and flocculation	This method is complex and inefficient, requiring alkaline additives for an optimal pH
Biological treatment	Micro-organisms are environmentally sensitive and difficult to control. Microbial cells can be destroyed by intermediates. This is a time-consuming and expensive method
Ultraviolet treatment	This is a costly method that can be disrupted due to water turbidity. This method is not efficient for the removal of heavy metals and other biological components
Reverse osmosis	The water used in this process is acidic. No volatile organic compounds, chemicals, chlorine, chloramines or drugs are removed using this method
Nanofiltration	Pre-treatment and high-water purification are required for this procedure. There is limited retention of salt and univalent ions
Ultrafiltration	This procedure requires large amounts of energy and does not remove dissolved inorganic substances
Microfiltration	Metal, fluorite, sodium, nitrates, organic volatility and dyes are not removed in this process. This process requires regular cleaning and membrane fouling
Carbon filter	Fluoride, nitrates, sodium, metals, etc., cannot be removed through this procedure. This can be moulded, and it is blocked by un-dissolved solids

Microbial agent

The membrane and cell wall are the main protective barriers to external bacterial resistance. The bacterial cell wall plays an essential role for preserving the bacteria's natural shape. There are different nanocomposite and gram-positive and gram-negative bacteria adsorbent cell membrane components. Lipopolysaccharides (LPS), a distinctive part of the gram-negative cell wall, provides a highly loaded area with nanocomposite characteristics. Teichoic acid, on the other hand, is reflected only in the cell wall of gram-positive bacteria so that nanocomposites are spread along the molecular chain of phosphates, stopping their aggregation. Many studies indicate that nanocomposites are more active than gram-negative bacteria against gram-positive bacteria because LPS, lipoprotein and phospholipids, are the gram-negative cell wall bacteria that build a binding barrier that enables only macromolecules to join. By comparison, a thin layer of peptidoglycan, as well as teichoic acid and abundant pores, is present in the cell wall of the gram-positive bacteria to allow the entry of foreign molecules that cause cell membrane damage and cell death. In fact, unlike gram-negative bacteria, gram-positive fungi have increased adversity to nanocomposite-containing cell surfaces. Depending on the part and components of the bacterial cell, nanocomposites cause bacterial mortality.

Nanotechnology was reported by Pelgrift and Friedman as offering therapeutic assistance with drug-resistant microbes (Pelgrift and Friedman 2013). Several nanoparticles in the medical community, agriculture, water resources and the environment are widely utilized as an antibacterial agent. Nanocomposites based on metal nanoparticles, metal oxide nanoparticles and green nanoparticles can overcome the limitations of conventional antibiotic drugs, such as difficulties in penetration and excretion from system after therapy. Nanocomposites that consider biofilm elimination inhibit growth by providing good adhesion to cells, acid production, quorum sensing and tolerance. Mechanisms involved in the bactericidal activity of nanoparticle-based nanocomposites include the generation of reactive oxygen species, the release of ions and the impact of the bacterial cell membrane. Iron oxide (I & III), zinc oxide, titanium dioxide, copper oxide, magnesium oxide, nickel oxide and calcium oxide exhibited promising results in antibacterial activity. Physicochemical properties of nanocomposites' shape, size, crystallinity, chemical composition, orientation, solubility and surface area play an important role in antibacterial activity (Ghorbi et al. 2019). In this paper, the antimicrobial activity results of nanocomposites are discussed in detail. These findings have shown that nanocomposites are a good antimicrobial agent compared to individual nanoparticles, possibly due to physical and chemical alterations.

Nanocomposites

Nanocomposites are solid multi-phase materials typically consisting of two or more physically distinct components and with one or more dimensions less than 100 nm with a noticeable interface between them. This description may be restricted to materials in a reinforcing stage for structural applications, including fibres or parts supported by a binder or matrix phase. Such materials have a wide range of applications, as they can combine various characteristics

according to particular requirements. As alternatives to conventionally filled polymers, nanocomposites constitute a new material class. This newly formed class of materials contains nanosized of inorganic fillers (in at least one dimension). Owing to their high surface area, high fraction of the surface atoms and various binding effects, the polymer characteristics are substantially improved compared to the equivalents in bulk sizes. That has contributed to new and enhanced qualities, such as high chemical resistance, heat resistance and tensile strength (Chou et al. 2010) as well as viscoelastic properties, thermal degradation and glass transition temperature (Christian et al. 2008). Some composites have shown themselves to be up to 1000 times stronger than their corresponding material components (Chou et al. 2010).

In the last 10 years, a number of polymer composite forms have become the prevalent class of multifunctional polymer systems, and these material classes have received widespread attention in research, marketing and production worldwide. Composites in such diverse fields as manufacturing, transportation, electronics and consumer goods are already commonly used and have shown an exceptional combination of weight, strength and stiffness, which are difficult to achieve separately in the individual components (Giannelis 1996). Nanocomposites exhibit considerably improved properties as opposed to pure polymers and classical composites because of their nanometre dispersion.

Types of nanocomposites

There are three main types of nanocomposites, as shown in Fig. 5.

Ceramic matrix nanocomposites

Composites in the ceramic matrix (CMCs) are ceramic fibres embedded in ceramic matrices. All ceramic materials consist of a matrix and fibres, including carbon fibres. Ceramics, which occupy most of the volume, often come from a group of oxides, such as borides, nitrides or silicates, while metal is often used as the second component. To generate other magnetic, optical and electrical properties, corrosion, tribological, resistance and other protective properties of both components must be finely dispersed (Zhang et al. 2003).

Metal matrix nanocomposites

Nanocomposites of the metal matrix may also be known as composites of a reinforced metal matrix. Such composite forms may be categorized as non-continuous and continuous materials. The carbon nanotube-metal matrix composite (CNT-MMC) is one of the most common nanocomposites. CNT-MMC is an emerging new material that is being developed to benefit from electrical conductivity and high carbon nanotube tensile strength (Janas and Liszka 2018). The commercially successful production of synthetic technologies will guarantee that nanotubes in a metal matrix are distributed homogenously. This results in good interfacial adherence between the metal matrix and the carbon nanotubes, which is necessary for a CNT-MMC with optimum characteristics in those areas.

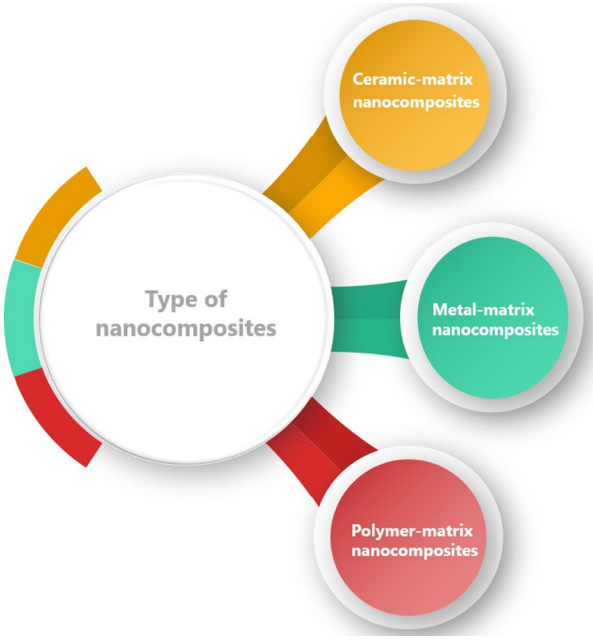

Fig. 5 Main types of nanocomposites

Polymer matrix nanocomposites

If nanoparticles are to be applied to a polymer matrix properly, their efficiency will also be dramatically improved by simply capitalizing on the nature and properties of a nanoscale filler (Manias 2007). This strategy is particularly successful in producing high-performance composites if the filler dispersion is achieved uniformly and the nanoscale filler has substantially varying or better characteristics than the matrix. The uniformity of the distribution is balanced by thermodynamically guided separation of the phase in all nanocomposites.

Synthesis modes for nanocomposites

Different methods are available to synthesize nanocomposites, and the choice of the synthesis method depends both on the nanoparticle and on the polymer used. All these methods can be divided into three different approaches. One approach is an *in-situ* metal polymer matrix by decreasing the metal salts in the matrix or by heating metals at the surface of the polymer. The polymerization of the matrix around the nanoparticles is another approach. The third approach is to combine pre-made NPs with pre-made polymer and enable complete synthetic

control of the matrix and nanoparticles. The addition to the polymer matrix of stabilized NPs is sensitive to both capped NP and the polymer matrix's relative molecular weight. The solubility of the polymer in water also depends on this. Many studies on the integration of water-soluble Ag NP into water-soluble matrices, including polyvinyl and acrylic acid, have been published (Penlidis; Akyildiz and Michielsen 2013; Ni et al. 2014; Fahmy et al. 2016). Moreover, the use of silver nanoparticles in hydrophobic polymers is much less studied. This is because the functional groups have no favourable interaction with silver nanoparticles, and therefore, melting techniques for nanocomposite formation with capped NPs are required. This is true for ester-functional polymers like polymethyl methacrylate.

Graphene oxide-based composites as a disinfectant

Due to the unique 2D assembly and associated band structure, graphene and graph-based composites have many advanced possible applications. Graphene has attracted the attention of many scientific innovations, as it has high electrical conductivity at room temperature (Zhu et al. 2019) (106 s cm^{-1}), an exceptionally large surface area (2630 m^2g^{-1}) (Stoller et al. 2008), good optical transmittance (~97.7%), excellent mobility as charge carriers (Bolotin et al. 2008) (~20 m^2 V^{-1} s^{-1}), good fracture strength (Lee et al. 2008) (125 GPa), good mechanical properties (Lee et al. 2008) (~1.1 TPa), a high breaking strength (Balandin et al. 2008) (42 N m^{-1}), superior thermal conductivity (~5000 W m K^{-1}) (Zhu et al. 2011; Song et al. 2019) specific magnetism, chemical stability and high carrier density (~1012 cm^{-2}) (Basu and Bhattacharyya 2012). Pure graphene is hydrophobic in nature and cannot be spread out in aqueous solutions, which limits its use for the purification of water (Li et al. 2008). Graphene and its composites are used in many different applications such as transistors, sensors, photonics, electronics, biotechnology, composite materials, storage and energy production. The large surface of graphene and its flexible functionality enable the adsorption of different impurities from aqueous matrices (Gurunathan et al. 2013; Kim et al. 2015); however, graphene's hydrophobicity and limited dispersibility decreases its potential for adsorbent purposes (Dubey et al. 2015). Various reports are available in the literature on improving the dispersibility of functional graphene through covalent or non-covalent attachments (Konkena and Vasudevan 2012; Dubey et al. 2015). The functionalization of graphene with metals and metal oxides further improved the water content and capacity for adsorption (Dubey et al. 2015).

Owing to the large hydrophilic groups (carboxylic, epoxydic and hydroxy groups) on their surface, GO is easily dispersed in water. GO has a strong hydrophilic group and a wide surface area and is considered a good adsorbent. GO's rapid dispersion into solutions and the adsorption of pollutants into stable complexes lead to problems with the separation and recovery of GO (Yu et al. 2015). An alternative approach is the magnetic functionalization of GO that is used to solve these separation problems (Zhu et al. 2011). Due to its specific characteristics, such as chemical stability, magnetic separation and the creation of stable complexes with pollutants, they are commonly used to remove pollutants of different types. Some researchers have successfully produced composites of magnetic graphic oxide for water treatment, energy storage and drug delivery (Singh et al. 2011; Gandhi et al. 2019).

Nevertheless, the use of graphene as an adsorbent is limited due to difficulties in filtration and reproduction. The use of magnetic water treatment materials can solve these problems, including filtering and regenerating adsorbents, and lead to the development and use of magnetic water purification materials (Reddy and Lee 2013). Because of the magnetic and chemical stability of the magnetic reverse spinel as well as its high-surface porous nature, it is widely used for water purification (Dhand et al. 2013; Song et al. 2019). The nano-metal ferrites are therefore poorly stable (Karim et al. 2008). Many researchers have used magnetic-carbon functional composites to recover and extract valuable metals (Muravyov et al. 2012) and magnetic organic composites (Zhao et al. 2013). GO can improve the adsorption of heavy metals due to its carboxylic, epoxy and hydroxyl functions (Li et al. 2009). In addition, composites made of MGO have demonstrated higher water treatment efficiencies (Koo et al. 2011).

Chandra et al. (2010) used the chemical reaction of superparamagnetic rMGO composites, which produced an average size of 10 nm. In both the elimination of As (III) and As (V), the composite displayed an adsorption efficiency of 99.9%. For the excellent adsorption of water-based arsenate, Zhang et al. used a ferric hydroxide-GO-composite (Zhang et al. 2010). The large adsorption of arsenate was found in this case in a spectrum of pHs (4–9) and reduced arsenate in polluted water from (20–0.5) ppm. The adsorption capacity declined as the pH increased to > 8; however, the leakage of treated water of < 1.0 ppm iron was observed. A copper-catalysed azide-alkyne cycloaddition was made from a water-soluble MGO nanocomposite and was used for the adsorption of Cd (II), Pb (II) and Cu (II) from the water system (Zhang et al. 2013). The findings revealed that the structure of the nanocomposite, its superparamagnetic properties and its outstanding complex potential are superior to the usual ability to extract heavy metals. The rGO-MnO_2 nanocomposites demonstrated an outstanding ability to remove mercury compared with its basic form. This approach also includes the inherent removal of RGO without external interventions, which leads to an easy and environmentally sustainable solution (Sreeprasad et al. 2011). The Fe_3O_4–rGO–MnO nanocomposite was designed for the adsorption of As (III) and As (V) (Luo et al. 2012). The findings of these studies indicated that the composite was

able to boost adsorption, which can be enhanced by reducing the MnO_2 and Fe_3O_4 aggregations. In their research, Liu et al. succeeded in removing Co (II) by MGO and found that the adsorption of Co (II) on MGO was rate limiting, resulting in surface complexation in the internal sphere (Liu et al. 2011). In the meantime, precipitation and interior surface complexation was found to be consistent with the removal of Co (II) at a higher pH. MGOs sorbed with Co (II) can easily be separated from an aqueous solution by using an external magnetic field (Liu et al. 2011). It has also been suggested that 3-aminopropyltrimethoxysilane can be effectively self-assembled with GO by electro-static interactions (Liu et al. 2013). The tests further revealed that the prepared MGO has a higher adsorption capacity than GO or Fe_3O_4 alone. In addition, the prepared MGO not only prevented the agglomeration of magnetic particles but also strengthened the composite structure, allowing the scattering of GO and Fe_3O_4 microspheres on the other side. A novel magnetic composite that consists of Fe_3O_4, rGO and polypyrrole (Ppy) nanoparticles (Ppy–Fe_3O_4/rGO) was synthesized for the adsorption of Cr (VI) (Wang et al. 2015). A higher maximum adsorption capacity for Cr(VI) was observed on Ppy–Fe_3O_4/rGO than Fe_3O_4/rGO.

Zhao et al. employed layered GO-based nano-sheets for U (VI) adsorption with a maximum adsorption capacity (q_{max}) of 97.5 mg/g (Zhao et al. 2012). Nevertheless, due to the aggregation of GO nano-sheets in the atmosphere, the adsorption efficiency of prepared nano-sheets was considerably reduced. The functionality of GO nano-sheets reduced and overcame the above constraint. Considering this, the functionalization of GO by magnetic materials can be regarded as a simple and efficient method for overcoming GO aggregation. Magnetic nanocomposites typically demonstrated high adsorption when radionuclides were selectively removed.

Many industries are currently using pigments and dyes for colouring their goods, including paper, fabrics, painting, plastics and leather. The presence of dyes in aquatic environments influences not only the appearance of aesthetics, but also inhibits the penetration of sunlight, thus reducing the photosynthesis of aquatic plants (Mokhtari et al. 2016). Therefore, before the discharge of effluent, these dyes must be effectively eliminated. Many researchers and scientists have developed strategies and corrective methods for eliminating this major concern. Methylene orange, methylene blue, malachite green, BR-1 2, Congo red, Orange Acid 8, Azo Acid Red 14, Yellow Acid 99, Persian orange, amido black 10B and orange Reactive 12 are among the common dyes found in wastewater and effluent. Many physicochemical methods for extracting these dyes from effluent water and wastewater have already been established such as photocatalytic degradation (He et al. 2017), separation by membrane (Bouazizi et al. 2017), the coagulation process (Li et al. 2016), electrolysis (Zou and Wang 2017), liquid–liquid extraction (Bukman et al. 2017) and adsorption (El Essawy et al. 2017). The aquatic ecosystem is also polluted by the agricultural discharge from fruits, rice, maize and vegetables. The use of excessive insecticides/pesticides results in contaminants from these discharges. Insecticides based on neonicotinoids are effective alternatives to the carbamates and organophosphates used in most countries to kill insects. Acetamiprid, thiacloprid, clothianidin, nitenpyram, dinotefuran, imidacloprid and thiamethoxam are popular neonicotinoid insecticides (Tian et al. 2016). The residue of these insecticides can contaminate soil, plants, vegetables and water in the environment, posing potential threats to human health and habitats due to long-term accumulation and widespread usage (Klarich et al. 2017). A macro-composite metal organ magnetic framework (MMOF) was used for a magnetic core and enabling the adsorption and removal of insecticide neonicotinoid pollutants using a Fe_4O_3–graphene oxide (GO)-ß- cyclodextrin nanocomposite (β-CD) (Liu et al. 2017). The adsorption capacities for 100 mg/L were found to be 1.77, 2.56, 2.88, 2.88, 23.86 and 3.11 mg/g for clothianidin, nitenpyram, thiacloprid, thiamethoxam, acetamiprid and imidacloprid, respectively. The results confirmed that neonicotinoid insecticides from agricultural wastewater are an excellent adsorbent of MMOF.

GO/rGO-based nanocomposites are found to be effective for antibacterial activities. Jaworski et al. (2018) synthesized an AgNPs-GO nanocomposite of NP size = 80 nm. The antimicrobial activity was performed on *E. coli*, *S. epidermidis*, *S. aureus* and *C. albicans*. It was observed that the inhibition % of *E. coli* was highest compared with the other three microbials. Ganguly et al. (2017) synthesized an AgNPs-GO nanocomposite of NP size = 60 nm. The antibacterial activity was performed on *E. coli* and *S. aureus*. Using a concentration of 10 (µg/mL), inhibition (%) of 100 was achieved for both *E. coli* and *S. aureus*. Hussain et al. (2014) synthesized an Au-rGO nanocomposite of NP size 50 = nm. The antimicrobial activity was performed on *S. aureus*/*B. subtilis* and *E. coli*/*P. aeruginosa*. It was observed that *S. aureus*/*B. subtilis* had a higher inhibition (%) than *E. coli*/*P. aeruginosa*. A detailed survey of GO/rGO-based nanocomposites' antibacterial properties is presented in Table 2.

Zinc oxide nanocomposites as disinfectant

ZnO is a semiconductor with a wide band gap energy of 3.37 eV at room temperature and is extensively used in electrical, catalytic, photochemical and optoelectronic applications. The composite of ZnO showed enhanced applications on the nanoscale. Esmailzadeh et al. (Esmailzadeh et al. 2016) synthesized nanocomposites by mixing ZnO with low-density polyethylene and performed antimicrobial activity on *Bacillus subtilis*, a common food spoiler bacterium, and *Enterobacter aerogenes* (food and water) produced on pathogens. Antibacterial effects were found to be more pronounced on

Table 2 GO/rGO-based nanocomposites' antimicrobial properties

S. No	GO-based nanocomposite	Bacteria model(s)	Findings	References
1	AgNPs-GO	*E. coli*, *S. epidermidis*, *S. aureus*, *C. albicans*	NP size = 80 nm, concentration = 200 (µg/mL), Inhibition (%), *E. coli* = 89, S. epidermidis = 76, *S. aureus* = 81, *C. albicans* = 78	Jaworski et al. (2018)
2	AgNPs-GO	*E. coli*/*S. aureus*	NP size = 60 nm, concentration (µg/mL) = 10, Inhibition (%) = 100	Ganguly et al. (2017)
3	AgNPs-GO	*E. coli*	NP size = 40 nm, concentration (µg/mL) = 6.4, Inhibition (%) = 100	Zhu et al. (2013)
4	AgNPs-GO	*E. coli*/*S. aureus*	NP size = 98 nm, concentration (µg/mL) = 6.4, Inhibition (%) = 100	Bao et al. (2011)
5	AgNPs-rGO	*E. coli*	NP size = 57 nm, concentration (µg/mL) = 40, Inhibition (%) = 100	Moghayedi et al. (2017)
6	AgNPs-rGO	*E. coli*	NP size = 12 nm, concentration (µg/mL) = 20, Inhibition (%) = 100	Zhou et al. (2013)
7	Au-rGO	*S. aureus*/*B. subtilis* *E. coli*/*P. aeruginosa*	NP size = 50 nm, concentration (µg/mL) = 250, Inhibition (%), *S. aureus*/B. subtilis = 94, *E. coli*/*P. aeruginosa* = 50	Hussain et al. (2014)
8	Cu_2ONPs-rGO	*E. coli*, *S. aureus*	NP size = 30 nm, concentration (µg/mL) = 40, Inhibition (%), *E. coli* = 70, E. *S. aureus* = 65	Yang et al. (2018)
9	TiO_2-GO	*E. coli*	NP size = 30 nm, concentration (µg/mL) = 180, Inhibition (%) = 100	Chang et al. (2015)
10	ZnO-GO	*E. coli*	NP size = 75 nm, concentration (µg/mL) = 500, Inhibition (%) = 100	Nourmohammadi et al. (2014)
11	Fe_2O_3-GO	*E. coli*	NP size = 225 nm, concentration (µg/mL) = 100, Inhibition (%) = 97	Santhosh et al. (2014)
12	Fe_3O_4-GO	*E. coli*	NP size = 66 nm, concentration (µg/mL) = 300, Inhibition (%) = 91	Deng et al. (2014)
13	Mn Fe_2O_4-GO	*E. coli*	NP size = 170 nm, concentration (µg/mL) = 100, Inhibition (%) = 82	Chella et al. (2015)

gram-positive bacteria. Motshekga et al. synthesized ZnO and bentonite-supported silver nanocomposites (Motshekga et al. 2015). *Faecalis* bacteria were used for performing the antibacterial activity. The synthesized nanocomposites showed good antibacterial activity. For the nanocomposites of ZnO, however, the best antibacterial activity showed at least 78 percent removal performance. Hazem et al. prepared a chitosan/silica/zinc oxide nanocomposite that was used to remove methylene blue (MB) from wastewater (Hassan et al. 2019). The adsorption process at pH 7 was demonstrated to be effective. The Langmuir model was found feasible for the adsorption process. On the other hand, Abdullah et al. prepared a zeolite/zinc oxide nanocomposite using a co-precipitation method (Alswata et al. 2017). The adsorption of arsenic As (V) and lead Pb (II) was performed under room pressure and temperature. The maximum removal of the toxic metals was found to be 89% and 93% for As (V) and Pb (II), respectively. According to the obtained results, a pseudo-second-order kinetic model and Langmuir isotherm were found to be best fitted to the experimental data. This technique was economic and effective for the removal of heavy toxic metals.

Archana et al. prepared graphene oxide decorated zinc oxide nanocomposites using a simple hydrothermal method (Archana et al. 2018). The resultant GO-ZnO nanocomposite showed an exceptional adsorption ability and the strong adsorption for the removal of methyl orange (MO) and MB from an aqueous solution. The pseudo-second-order kinetic was found to be a feasible process for adsorption. Naseem et al. prepared a reduced graphene oxide/zinc oxide (rGO/ZnO) nanocomposite using a chemical method (Naseem et al. 2020). The photocatalytic degradation of MB was 80% after 5 h. The 4-nitrophenol (4-NP) was reduced to 4-aminophenol (4-AP) in three minutes in the presence of a reducing agent ($NaBH_4$) and 10 min in the absence of a reducing agent. Furthermore, they also successfully performed antibacterial activity on three bacteria: *Escherichia coli*, *Pseudomonas aeruginosa* and *Staphylococcus aureus*.

Ahmed et al. synthesized ZnO/graphene composites using the single-step solvothermal method (Ahmad et al. 2013b). The prepared nanocomposite attained almost 100% degradation in just 90 min in under visible light irradiation. Sani et al. prepared zinc oxide/clay mineral nanocomposites using a simple green heating method (Sani et al. 2016). The percentage removal of ZnO/MMT was found to be 89.5% (Cu) and 97.2% (Pb), which were much higher than 80.6% (Cu) and 90.3% (Pb) for ZnO/talc. Table 3 provides a thorough

analysis of the nanocomposites based on ZnO and their wastewater treatment method.

Copper oxide nanocomposites

CuO-based nanocomposites, because of their high electrochemical capabilities (Table 4), have different technical applications such as in batteries and catalysis (Borgohain and Mahamuni 2002). Li et al. proposed a biochar-supported copper oxide (BC-CuO) nanocomposite for the treatment of highly saline (100–400 mM) wastewater (Li et al. 2020). The rapid removal of methylene blue (MB), ciprofloxacin, atrazine, acid orange 7 and rhodamine B were observed within 30 min, with high efficiencies of 78.27%, 99.68%, 100%, 100% and 100%, respectively. Majdalawi et al. synthesized a nanocomposite comprised of silica and copper oxide (SiO_2/cuO) by the dissolution of SiO_2 in 6.0 M NaOH followed by the deposition of dissolved SiO_2 on CuO (Majdalawi and Krishan 2019). The synthesized SiO_2/CuO showed an exceptionally fast rate of adsorption for the CV and MB, where, within 1 min, 66% and 77% of the initial amounts were removed, respectively. Qu et al. synthesized Cu-AC (AC: activated carbon) and Cu/Ce-AC nanocomposites using a one-pot sol–gel method (Jun-e et al. 2017). The synthesized Cu/Ce-AC achieved over 97% COD and 80% TOC removals in just 50 min. The high electric catalytic efficiency of the Cu/CE-AC material makes this nanocomposite promising for the electrochemical treatment of organic pollutants in an aqueous solution. A thorough analysis of CuO-based nanocomposites and their use for wastewater treatment is presented in Table 5.

Silver/silver oxide nanocomposites

To fulfil the diverse requirements of biomedicine, silver and its nanocomposites have received increased attention (Tables 6, 7, 8). Silver nanoparticles are typically smaller than 100 nm in silver-based nanocomposites and contain 20 to 15,000 silver atoms. Silver nanoparticles are highly affected by their shape and size due to their catalytic, thermal, and optical properties. Additionally, due to their broad-spectrum antimicrobial ability, the most popular sterilizing materials used in food storage and medical items are also silver nanoparticle-based composites, for instance, personal care products, food storage bags, textiles and refrigerator surfaces. The effects of different silver nanoparticle (AgNP) ratios on the systemic dose of GO's and nanocomposite antibacterial activity have been investigated systematically. Our findings show that even at very low concentrations (2.5 µg/ml), GO-Ag nanocomposites with the best AgNP-GO ratio show a significant comparison with simple AgNPs or AgNP mixtures. The antibacterial activity was increased because of its unique physicochemical characteristics. Modifications in morphology and bacterial cell division were studied to examine the antibacterial mechanism of GO-Ag nanocomposites. It is interesting that *Escherichia coli* is more toxic to GO-Ag nanocomposites. Mauter et al.'s research provided a detailed understanding of GO-Ag nanocomposites' antimicrobial behaviour and emphasized their potential as a powerful antimicrobial agent (Mauter and Elimelech 2008). Graphene-Ag/Zn nanocomposite was made by means of a non-hazardous solvothermal procedure for the photodegradation of organic dyes. At the time of reaction, the filling of silver doped zinc oxide nanoparticles on two-dimension graphene sheets was attained. This research provided a new method for the in situ fabrication of the graphene Ag–ZnO nanocomposite, and its photocatalytic performance is highly efficient for the removal of dyes (Ahmad et al. 2013a).

The optical, structural and morphological properties of AgI nanocomposites were studied when a graphene nanostructure was supported on a silver iodide nanostructure. Under visible light, AgI nanocomposites are used for the elimination of organic dyes such as rhodamine B. The result indicated that silver iodide decorated with graphene showed greater photocatalytic activity than undecorated silver iodide. Therefore, the maximum visible-light photodegradation efficiency marked the silver iodide-reduced graphene oxide as an excellent material for the elimination of organic dye from wastewater and is capable of being used in near-UV white LEDs (Reddy et al. 2015). The synthesized Ag–Cu_2O/rGO nanocomposites had a high photocatalytic performance for the removal of dyes such as MO, and its degradation rate was higher than the original cuprous oxide and cuprous oxide/reduced graphene oxide nanocomposites. This research showed unprecedented photocatalytic efficiency for the degradation of a phenol solution for the first time by using silver-based cuprous oxide/rGO nanocomposites and its higher photocatalytic activity (Sharma et al. 2018).

Silver titanium dioxide/rGO nanocomposite was synthesized using a single-step method using titanium oxide nanoparticles, $AgNO_3$, and GO without any reducing agents. This method provides the remarkable benefits of the one-step method without using poisonous reagents or reducing agents to produce the nanocomposite of Ag–TiO_2/rGO. Due to high photocatalytic reduction, antibacterial activity and an easy method, the silver titanium dioxide/rGO nanocomposite is an outstanding material for wastewater treatment. Silver titanium dioxide/rGO nanocomposite showed higher photocatalytic degradation compared to any other synthesized photocatalysts (Pant et al. 2016). Huang et al. synthesized GO/Ag nanocomposite with different Ag loading using a facile solution-phase method. In the synthesis, the direct reduction of $AgNO_3$ on a GO matrix was carried out (Huang et al. 2016). The synthesized nanoparticles showed better antibacterial activity against *Escherichia coli* and *Staphylococcus aureus*. Silver nanoparticles (AgNPs) functionalized with either graphene oxide (GO) or lactoferrin (LTF)

Table 3 ZnO-based nanocomposites and their applications for wastewater treatment

S. no.	ZnO-based nanocomposite	Application	Findings	References
1	Chitosan/silica/zinc oxide	Adsorption: dye removal (methylene blue (MB))	NP diameter = 50 nm Highest adsorption capacity = 293.3 mg/g Maximum adsorption capacity at pH 7 Best fitted model(s) = Langmuir isotherm	Hassan et al. (2019)
2	Zeolite/zinc oxide	Adsorption: lead Pb (II) and arsenic As (V)	NP diameter = 4.5 nm Highest adsorption capacity, Pb (II) = 93% and As (V) = 89% Maximum adsorption capacity at pH 4 Best fitted model(s) = Langmuir isotherm and pseudo-second-order kinetic	Alswata et al. (2017)
3	Graphene oxide-zinc oxide (GO-ZnO)	Photodegradation activity: methylene blue (MB) and methyl orange (MO)	NP sizes = 100–200 nm Highest adsorption capacity, MB = 265.95 mg/g and MO = 714.28 mg/g Maximum adsorption capacity at pH 7.4 Best fitted model(s) = Langmuir isotherm	Archana et al. (2018)
4	Reduced graphene oxide/zinc oxide (rGO/ZnO)	Photodegradation activity: methylene blue and 4-nitrophenole	NP sizes = 25–30 nm Highest adsorption capacity, MB = 80% and 4-NP = 100%	Naseem et al. (2020)
5	Graphene oxide/zinc oxide	Photodegradation activity: methylene blue (MB)	NP size = 70 nm Highest adsorption capacity, MB = 98.17% Maximum adsorption capacity at pH 8.2 Best fitted model(s) = pseudo-second-order kinetic	Hosseini (2016)
6	Chitosan-zinc oxide (CS/ZnO)	Photodegradation activity: dye removal (methylene blue (MB))	NP size = 259.6 nm Highest adsorption capacity, MB = 18 mg/g Maximum adsorption capacity at pH 6.4 Best fitted model(s) = Langmuir isotherm	Bagavathy et al. (2019)
7	Polyaniline/ZnO	Adsorption: Cr (VI)	NP size = 31.2 nm Highest adsorption capacity, Cr (VI) = 36 mg/g Maximum adsorption capacity at pH 2 Best fitted model(s) = Langmuir isotherm and pseudo-second-order kinetic	Ahmad (2019)
8	Silica/zinc oxide (ZnO/SiO_2)	Adsorption: hydrogen sulphide	NP size = 10.55 nm Highest adsorption capacity = 100% Maximum adsorption capacity at pH 12 Best fitted model(s) = Freundlich isotherm and pseudo-first-order kinetic	Nemati et al. (2019)
9	ZnO/graphene	Photodegradation activity: methylene blue (MB)	NP size = 16–22 nm Highest adsorption capacity = 97.2%	Ahmad et al. (2013b)
10	Zinc oxide/natural-zeolite	Adsorption: penicillin	NP size = 91 nm Highest adsorption capacity = 100% Best fitted model(s) = Freundlich isotherm and intra-particle diffusion kinetic	Khosravian et al. (2017)

Table 3 (continued)

S. no.	ZnO-based nanocomposite	Application	Findings	References
11	Zinc oxide/polypyrrole nanocomposite	Adsorption: brilliant green	NP size = 10 nm Highest adsorption capacity = 140.8 mg/g Best fitted model(s) = Langmuir isotherm and pseudo-second-order kinetic	Zhang et al. (2019b)
12	Zinc oxide/clay minerals nanocomposite	Adsorption: Cu(II) and Ph(II) ions	Highest adsorption capacity, Cu(II) = 83.30 mg/g and Ph(II) = 88.50 Maximum adsorption capacity at pH 4 Best fitted model(s) = Langmuir isotherm	Abubakar (2020)
13	MgO-ZnO/carbon nanofiber nanocomposite	Extraction and preconcentration of CBZ from wastewater	NP size = 36.3 nm (ZnO), 26.9 nm (MgO) and 12.3 nm (CNFs) Highest adsorption capacity = 95.8% Maximum adsorption capacity at pH 6.5	Lekota et al. (2019)
14	Zinc oxide-coated nano porous carbon sorbent	Adsorption: Pb (II)	NP size = 3.8 nm Highest adsorption capacity = 522.8 mg/g, 97.25% Maximum adsorption capacity at pH 6 Best fitted model(s) = pseudo-first-order kinetic	Zolfaghari et al. (2013)
15	Zinc oxide/talc nanocomposite	Adsorption: Pb (II)	Highest adsorption capacity = 48.3 mg/g Best fitted model(s) = pseudo-second-order kinetic	Sani et al. (2016)
16	Chitosan-ZnO nanocomposite	Adsorption: reactive black HN and reactive magenta HB	Highest adsorption capacity = 99% Maximum adsorption capacity at pH 6	Sabrin (2015)
17	Al-doped ZnO	Adsorption: methylene orange (MO)	NP size = 20–30 nm Highest adsorption capacity = 98.65 mg/g Best fitted model(s) = pseudo-second-order kinetic and Langmuir isotherm	Wu et al. (2016)
18	Cu-doped ZnO nanocatalyst	Adsorption: amaranth dye	NP size = 50 nm Highest adsorption capacity = 63% Maximum adsorption capacity at pH 6	Pandian et al. (2018)
19	Zinc oxide-doped prussian blue nanocomposite	Photocatalytic degradation: toxic phenols	NP size = 100 nm Highest adsorption capacity = 97.25% Maximum adsorption capacity at pH 6.5	Rachna (2020)

were also reported (Suleman Ismail Abdalla et al. 2020). The antimicrobial activity for both the synthesized nanocomposites was performed against *P. aeruginosa*, *Staphylococcus aureus*, *Bacillus Sp*. and *Escherichia coli*. It was found that Ag-LFT showed much stronger antibacterial activity against *P. aeruginosa*. Alsharaeh et al. synthesized silver nanoparticles (AgNPs) and AgNPs/reduced graphene oxide (RGO) nanocomposites using lemon juice under UV and microwave irradiation (Alsharaeh et al. 2017). The antibacterial properties of AgNPs/RGOs have been studied in gram-negative bacteria. Table 4 presents a detailed review of existing Ag/AGO-based nanocomposites and their applications for the treatment of wastewater.

Titanium oxide nanocomposites

In recent years, the usage of photocatalysts for the drug degradation of TiO_2/G and TiO_2/GO nanocomposites has increased. The use of TiO_2/G nanocomposites developed by the microwave hydrothermal method with UV-A light radiation (Amalraj Appavoo et al. 2014) and TiO_2/G aerogels

Table 4 ZnO-based nanocomposites' antimicrobial properties

S. No	ZnO-based nanocomposite	Bacteria model(s)	Findings	References
1	Graphene oxide-zinc oxide (GO-ZnO)	*S. aureus*, *B. subtilis*, *P. aeruginosa, E. coli* and two strains of fungi namely *C. albicans and A. flavus*	NP sizes = 100–200 nm, concentration = 100 (µg/mL), minimum inhibitory concentration (MIC), *E. coli* = 5.25, *P. aeruginosa* = 6.5, *S. aureus* = 11.5, *B. subtilis*, *C. albicans* = 23 and *A. flavus* = 25	Archana et al. (2018)
2	Reduced graphene oxide/zinc oxide (rGO/ZnO)	*Escherichia coli, Pseudomonas aeruginosa* and *Staphylococcus aureus*	NP sizes = 25–30 nm, concentration, *P. aeruginosa* = 12, 14, 18 and 18 (µg/mL), = 16, 18, 20, 22 (µg/mL), *E. coli* = 500, 520 540, 560 (µg/mL) Maximum inhibition zone, *S. aureus* at 18 (µg/mL), *S. aureus* at 22 (µg/mL) and *E. coli* at 560 (µg/mL)	Naseem et al. (2020)
3	Chitosan-zinc oxide (CS/ZnO)	*Escherichia coli*, *Bacillus sp.*	NP sizes = 259.6 nm, Maximum inhibition zone, *Escherichia coli* at 120 (µl) and *Bacillus* sp. at 100 (µl)	Bagavathy et al. (2019)
4	Chitosan-based zinc oxide with MMT K_{10}	*S. Pneumonie*, *Escherichia coli* and *Klebsiella Planticola*	NP sizes = 151–165 nm, Maximum inhibition zone was at 100 (µl) by *S. Pneumonie*, *Escherichia coli* and *Klebsiella Planticola*	Annamalai et al. (2018)
5	Polyethyleneimine (PEI)-modified graphene quantum dot (GQD) and ZnO nanocomposite	*Escherichia coli*	NP sizes = 6.8 nm, Concentration 2 mg/mL	Liu et al. (2019)
6	ZnO polyurethane nanocomposite (ZPN)	*Escherichia coli*, *Bacillus subtilis*	NP sizes = 20 nm, Inhibition (%), *Escherichia coli* = 100 and *Bacillus subtilis* = 100	El Saeed et al. (2015)
7	Bentonite-supported zinc oxide nanoparticles	*Escherichia coli*, *Enterococcus faecalis*	Pore size = 17.96 nm, surface area = 3.1812 m^2/g, Inhibition (%), *Escherichia coli* = 100 and *Enterococcus faecalis* = 100	Motshekga et al. (2015)
8	ZnO–CuO	*E. coli* and *S. aureus*	NP sizes = 10–40 nm, Highest inhibition zone (mm) = 9 on E. coli	Rajith Kumar et al. (2020)
9	ZnO/SiO_2	*Escherichia coli*	NP sizes = 71.7 nm, Inhibition (%), *Escherichia coli* = 99	Shimada et al. (2020)
10	ZnO/TiO_2	*Escherichia coli, S. aureus*	NP sizes = 50–90 nm, *S. aureus* more susceptible than *Escherichia coli*	Pang et al. (2019)

Table 5 CuO-based nanocomposite methods and their use for wastewater treatment

S. No	CuO-based nanocomposite	Application	Findings	References
1	BC-CuO	Adsorption: acid orange 7, methylene blue (MB), ciprofloxacin, rhodamine B and atrazine	Average pore sizes = 2–50 nm, Maximum efficiency, methylene blue (MB) = 99.68%, acid orange 7 = 100%, rhodamine B = 7 = 100%, atrazine = 7 = 100% and ciprofloxacin = 78.27%	Li et al. (2020)
2	Cu-AC (AC: activated carbon) and Cu/Ce-AC	Electrochemical degradation: phenol	Average pore sizes = 2.098 nm, surface area = 816.957 m^2/g, pore volume = 0.392 cm/g Maximum efficiency, phenol = 97%	Jun-e et al. (2017)
3	Copper oxide nanowires decorated on activated carbon (AC@CuO-NWs)	Adsorption: methylene blue (MB)	Average crystalline size = 17.48 nm Maximum removal capacity at 328 K of 141.73 mg/g Best fitted model(s) = Langmuir isotherm Adsorption process nature = physisorption and endothermic	Lakkaboyana et al. (2019)
4	Zinc oxide/copper oxide (ZnO/CuO)	Photodegradation activity: direct red 80 azo dye	Maximum degradation 97.95 in 60 min	SILVA et al. (2015)
5	Monoclinic CuO/RGO	Photocatalytic activity: ortho and para nitrophenols (NP)	Average crystalline size = 19.3 nm Maximum degradation capacity at 100%	Botsa and Basavaiah (2018)
6	Kaolinite coated with copper oxide	Adsorption: lead (Pb^{2+}) ions	Particle size(s) = 0.600–20.01 (µm) Maximum adsorption at pH = 6.05 surface area = 47.01 (m^2/g)	Egirani et al. (2019)
7	Copper oxide-graphene oxide (CuO–GO)	Hydrogenation of nitroaromatics in water	Average crystalline size = 10 nm Maximum removal capacity 100% in 30 min	Zhang et al. (2019a)
8	CuO@Ag	4-NP reduction	Surface area 8.03 $m^2\ g^{-1}$, NP sizes = 50 nm, Concentration of 0.20 mg L^{-1} gives the best results	Bouazizi et al. (2018)

with the use of the hydrothermal method was successful in removing carbamazepine from water (Nawaz et al. 2017). Photodegradation was used for the nanocomposites TiO_2/G and TiO_2/Fe both through the application of visible and UV light irradiation for three pharmaceuticals: carbamazepine, antibacterial sulfamethoxazole and anti-inflammatory ibuprofen. TiO_2/G nanocomposites demonstrated higher UV light photocatalytic activity due to a decreased recombination rate between electron–hole pairs. TiO_2/Fe, however, showed greater photodegradation under visible light radiation as a result of the efficient reduction of the band gap (Lin et al. 2017a). However, with the immobilization on the optical fibre of TiO_2/G nanocomposites, photocatalytic degradation of the three aromatic drugs with aqueous solutions improved (Lin et al. 2017b).

Two TiO membrane preparation procedures were compared by Madaeni et al. (Madaeni et al. 2011). Firstly, PAA-PVDF membranes were created by grafting polymerization reaction during aqueous phases using the green chemistry process. TiO-NPs (20 nm) were self-assembled on the surface of the prepared PAA-PVDF by dipping the membranes at 0.05 wt% of the TiO_2 colloidal suspension. Eventually, for binding nanoparticles of TiO_2 on the surface of the hydrophobic PVDF membrane, the membranes were radiated by UV light (160 W). In the second procedure, the acrylic acid monomer was added at 0.05 wt% of TiO followed by the addition of an initiator and a liaison reagent. This reactive solution was treated with PVDF membranes; then, the same technique was applied as the first step (Amini et al. 2016). Also, nanoparticles of metal oxides played an important role in various oxidation reactions as a catalyst. They showed high catalytic reactivity to pollutant molecules and transformed these pollutants into environmentally friendly products (Soppe et al. 2014). Some special characteristics such as nano size, strong reactivity and a larger surface area are found in these nanomaterials. In particular,

Table 6 CuO-based nanocomposite's antimicrobial properties

S. no.	CuO-based nanocomposite	Bacteria model(s)	Findings	References
1	Chitosan/CuO nanocomposites	*Staphylococcus aureus* and *Escherichia* coli	NP size(s) = 41.02 nm, Highest inhibition zone (mm) = 9 on *Escherichia* coli and 9.5 on *Staphylococcus aureus*	Siriphannon and Iamphaojeen (2018)
2	Copper-chitosan Nanocomposites	*Shigella sonnei*, *Escherichia coli*, *Salmonella* typhi, *Pseudomonas aeruginosa*	NP sizes = 51–62 nm, Highest inhibition zone (mm) = 8.5 on *Escherichia coli* and 8 on *Shigella sonnei* and *Salmonella typhi* and rest were less than 8	Syame et al. (2017)
3	CuO@Ag	*Staphylococcus aureus*	Surface area 8.03 $m^2 g^{-1}$, NP size(s) = 50 nm, Concentrations (from 0.12 to 200 µmol mL^{-1})	Bouazizi et al. (2018)
4	CuO/C	*Escherichia coli, Pseudomonas aeruginosa, Klebsiella pneumoniae and Staphylococcus aureus, Aspergillus Niger and Candida albicans*	NP size(s) = 7–11 nm, Concentration (mg/ml) = 0.25, 0.5 and 1.0, Maximum zone of inhibitions at 1.0 mm, *Escherichia coli* = 11 mm, *Pseudomonas aeruginosa* = 12 mm, *Klebsiella pneumoniae* = 14 mm, *Staphylococcus aureus* = 11 mm, *Aspergillus Niger* = 13 mm, *Candida albicans* = 14 mm	Bhavyasree and Xavier (2020)
5	CuO–NiO	Antimicrobial activity: candian albicans	Average crystallite size = 39.34 nm MIC range = 0.97–15.62	Rahdar et al. (2017)

the removal of various impurities from surface water is a crucial part of TiO_2 photocatalysis. Many researchers have used photodegradation under many different conditions, e.g. UV or visible light choices, doped or undoped nanoparticles, metal/non-metal doping, etc., by different pollutant types such as organic pesticides, organic dyes or pharmaceutical products.

Gayathri et al. synthesized a TiO_2-graphene (TG) nanocomposite by uniformly distributing TiO_2 nanoparticles on graphene (Gayathri et al. 2015). TG nanocomposite demonstrated higher photocatalytic efficiency than bare TiO_2 nanoparticles and other composites. Enhanced composite behaviour is due to the reduction of the recombination of charge and organic dyes' interaction with graphene. Karimi et al. synthesized a nanocomposite of mesoporous titanium dioxide with MoS_2 nanosheets (MoS_2/TiO_2) (Karimi 2017). The synthesized nanocomposite MoS_2/TiO_2 exhibited outstanding photocatalytic activity for direct green 6 azo dye degradation under sunlight irradiation. The achieved photocatalytic performance by MoS_2/TiO_2 was about 2.2 times higher than mesoporous TiO_2. Table 9 presents a detailed review of existing TiO_2/TiO_2-based nanocomposites and their applications for wastewater treatment (Table 10).

Discussion

The global availability of pure water needs to be high to fulfil all current and predictable water requirements. There are many areas in which the drinking water available is insufficient to meet basic, economic and domestic development needs. For these regions, there are negative impacts on human health and the health of other living things due to inadequate freshwater to meet human needs and sanitation requirements. Research institutes/scientific societies must find ways to address these constraints. In addition, the world is currently facing many environmental challenges, particularly in view of a fluctuating and uncertain future climate, a rapidly growing population, urbanization and globalization. It is unclear how these problems, which include exploring all facets of water management, will be overcome. The use of nanomaterials for the treatment of water pollution in this modern era is increasing rapidly in order to meet poor water conditions and the high demand for freshwater worldwide. Innovative advanced water treatment approaches to certify high-grade water for drinking, eliminating micro-/macro-pollutants and enhancing industrial production by flexibly modifying water treatment methods are necessary. Nanotechnology has proven to be

Table 7 Ag/AGO-based nanocomposites and their various applications for wastewater treatment

S. no	Ag/AGO-based nanocomposite	Application	Findings	References
1	Ag/reduced graphene oxide nanocomposite	Adsorption: 4-Nitro phenol	Mean diameter of NP = 8.6 nm Maximum removal capacity of 100% was achieved in 12 min Best fitted model(s) = pseudo-first-order kinetics Activation energy = 43.7 kJ/mol	Hsu and Chen (2014)
2	Ag/ZnO	Photodegradation activity: methylene blue (MB)	Maximum removal capacity of 100% was achieved in 20 min	Ziashahabi et al. (2019)
3	Ag–Cu_2O nanocomposite	Photodegradation activity: methylene orange (MO)	Average diameter of NP = 22 nm Maximum removal capacity of 90% was achieved in 60 min	Sharma et al. (2018)
4	AgO/MgO/FeO@ Si_3N_4 nanocomposite	Adsorption of tetracycline (TC)	Average crystallite size = 2.85 nm Maximum adsorption capacity = 172.41 mg/g Maximum adsorption at pH = 8 Best fitted model(s) = Freundlich isotherm, pseudo-second-order kinetics	Sharma et al. (2020)
5	Fe_3O_4–Ag^0 Nanocomposites	Adsorption of mercury	Average diameter of NP = 23–41 nm	Inglezakis et al. (2020)
6	Silver-Graphene Oxide nanocomposite	Adsorption of anionic dye	Best fitted model(s) = Langmuir isotherm Physical adsorption	Jeyapragasam (2016)
7	Silver/quartz nanocomposite	Removal of mercury (II) ions	Average pore size = 5.78 nm Maximum removal at pH = 6 Best fitted model(s) = Langmuir isotherm, pseudo-second-order kinetics The adsorption of composite was a feasible, endothermic and spontaneous process	El-Tawil et al. (2019)
8	GO-Ag	Photodegradation of methylene blue dye	Average particle size = 18 nm Maximum degradation capacity of 100% was achieved in 30 min	Kumari et al. (2020)
9	Ag-TiO_2/rGO nanocomposite	Photodegradation of methylene blue, reactive black 16, and reactive orange 05	Average particle size = 21 nm Surface area = 50 ± 15 m2 g^{-1} Maximum removal capacity of 100% was achieved in 45–90 min	Pant et al. (2016)

highly successful in addressing water purification problems and progress will continue to be made in the future.

Approaches involving nanomaterials such as nano-sorbents and nanostructured catalytic membranes are highly effective, time-intensive, energy-efficient, and eco-friendly, but not all these methods are inexpensive. Also, they are not yet being used for commercial purposes in large-scale wastewater purification. It was also found that titanium was used in a packed bed reactor as an adsorbent to extract arsenic from water. Sand-coated iron oxide is used to extract arsenic from drinking water in some developing countries. As they display excellent physical, electrical, and chemical properties, various nanomaterials such as magnetic and carbon nanotubes can be used as sensor components. These sensors can allow water quality to be closely monitored. Nanomaterial sensors are used to detect various pollutants since they have optical properties that allow the sensors to detect pollutants more selectively and sensitively. Environmental pollution is caused by water pollutants, but the nanomaterials on polymer help protect the environment. Research has shown that nano-clay incorporation could be accomplished in the purification of water with polymer content. The reduction of hydrophobia helps to encourage the properties of nanocomposites. The benefits from the nanomaterial integration of nano-clay particles are evident for applications in humid environments. Owing to the special properties of nanocomposites, researchers have compared different synthesis methods to create novel nanocomposites. The synthesis technique plays an important role in producing a broader output and in regulating the nanocomposite quality. At the same time, the methods for environmental protection should be effective, affordable and safe.

Table 8 Ag/AgO-based nanocomposite's antimicrobial properties

S. no.	Ag/AGO-based nanocomposite	Bacteria model(s)	Findings	References
1	Polymer/silver Nanoparticle Nanocomposite	*Escherichia coli* and *Staphylococcus aureus*	Average particle size = 35–50 nm Ag-NP (M)/PVB average inhibition zones, *Escherichia coli* = 1.93, *Staphylococcus aureus* = *1.59*	Domènech et al. (2013)
2	Chitosan–silver oxide nanocomposite	*Escherichia coli, S. aureus, Bacillus subtilis and Pseudomonas aeruginosa*	Inhibition zones (mm), *Escherichia coli* = 16, *B. subtilis,* = 20, *Pseudomonas aeruginosa* = 24, *S. aureus* = 23	Tripathi et al. (2011)
3	Ag NPs/GO nanocomposite	*Escherichia coli* and *Staphylococcus aureus*	Average particle size = 5–20 nm Highest diameter of inhibition zone (DIZ) was observed for GO-Ag = 8 mL for both *Escherichia coli* and *Staphylococcus aureus*	Huang et al. (2016)
4	AgGO and Ag-LFT	*P. aeruginosa*, *Staphylococcus aureus, Bacillus* sp. and *Escherichia coli*	Average particle sizes, AgNP = 121.5 nm, AgGO = 354.0 nm and Ag-LFT = 130.8 nm Highest diameter of inhibition zones of Ag-LFT are, *S. aureus* = 13.5, *Bacillus* = 11.9, *P. aeruginosa* = 12.9 and *E. coli* = 14.0	Suleman Ismail Abdalla et al. (2020)
5	AgNPs/rGO nanocomposites	*Escherichia coli*	Average diameter = 3–8 nm AgNPs and AgNPs/RGO nanocomposites showed an inhibition zone of the 5 wt% AgNPs/RGO nanocomposites that are similar to neat AgNPs	Alsharaeh et al. (2017)
6	Ag-GO Nanocomposite	*Escherichia coli*, *P. aeruginosa*, *S. aureus*	Average particle size = 41–60 nm Diameter of inhibition zone (DIZ) (mm) of *Escherichia coli* = 18, *P. aeruginosa* = 18 and *S. aureus* = 20, Minimum inhibitory concentration (MIC) (μg/mL) of *Escherichia coli* = 25, *P. aeruginosa* = 15 and *S. aureus* = 10	Khorrami et al. (2019)
7	Ag-TiO_2/rGO nanocomposite	*Escherichia coli*	Average particle size = 21 nm Surface area = 50 ± 15 m2 g^{-1} Nanocomposite showed good antibacterial activity on *E. Coli*	Pant et al. (2016)

This review paper is focused on the utilization of various nanocomposites for the removal of different forms of impurities from water and for antimicrobial properties. The differences in the concentrations of nanomaterials, synthesis processes, methods for antibacterial analysis, photodegradation or adsorption process methods and other differences make it difficult to compare nanocomposites for their effectiveness in antimicrobial and wastewater treatment. In the literature, most of the nanocomposites were formed with graphene oxide and metal oxide nanoparticles. The graphene oxide nanocomposites were found to be more effective for antimicrobial activities and showed better metal removal capabilities. Silver nanoparticle-based nanocomposites are more effective than other nanocomposites for both antimicrobial and wastewater treatment. Photocatalytic nanoparticles (like ZnO and TiO_2)-based nanocomposites are also effective for removing heavy metals and have shown better antimicrobial effects than Ag-based nanocomposites. In addition, a mixture of different NPs and metal oxide NPs have been produced in many multi-component materials, resulting in greater anti-microbial activity and better adsorption or photodegradation than individual components because of a synergetic effect.

The antimicrobial properties of nanocomposites were mostly tested with *Staphylococcus Aureus* and *Escherichia coli* as microorganisms. Ongoing research needs to focus

Table 9 TiO_2-based nanocomposites and their applications for wastewater treatment

S. no.	TiO_2-based nanocomposite	Application	Findings	References
1	MoS_2/TiO_2	Photodegradation activity: direct green 6 azo dye	Pore diameter = 20 nm Surface area = 176.4 m^2/g The photodegradation by nanocomposite was 2.2 times higher than mesoporous TiO_2	Karimi (2017)
2	Titanium dioxide/polyethylene glycol (TiO_2/PEG PNC)-nanocomposite	Adsorption: ^{134}Cs and ^{60}Co	Average pore size = 20 nm Maximum removal at pH = 8 Best fitted model(s) = pseudo-second-order kinetics The adsorption of composite was favourable and endothermic	Sh and Zahra (2020)
3	Smectite-titanium oxide nanocomposite	Adsorption: As(III) and As(V)	Average pore size = 8.5–9.4 nm Maximum removal at pH = 7	Ebina et al. (2015)
4	Kaolinite/TiO_2/cobalt(II) tetracarboxymetallophthalocyanine nanocomposites	Photodegradation activity: photocatalysts for decomposition of organic pollutants trimethoprim, caffeine and prometryn	Maximum removal at pH = 12 Maximum degradation capacity = 90%	da Silva et al. (2019)
6	TiO_2-graphene oxide (TiO_2-GO) nanocomposite	Photodegradation activity: photocatalytic degradation of butane	Average pore size = 32–52 nm Best fitted model(s) = pseudo-first-order kinetics	Štengl et al. (2013)
7	ZnS–TiO_2/RGO ternary composites	Photodegradation activity: methylene blue	Maximum degradation capacity = 90% in 60 min	Qin et al. (2019)
8	Zinc oxide and titanium oxide nanostructures	Photodegradation activity: methyl orange (MO)	Average diameter = 20–40 nm Maximum degradation capacity = 90%	Gunti (2017)
9	Zeolite-titanium dioxide nanocomposites	Adsorption: P(V)	Mean crystallites size = 4 nm Maximum degradation capacity = 99.48%	Kravchenko et al. (2016)
10	Titanium-tin oxide nanocomposite	Adsorption: lead ions (Pb^{2+})	Average diameter = 34 nm Maximum adsorption capacity = 70.07 mgg^{-1} Best fitted model(s) = Langmuir isothermal	Mahfooz-Ur-Rehman et al. (2019)
11	TiO_2/G and TiO_2/GO	Photodegradation activity: methylene blue, fulvic acid, bromate	Average pore size = 1–10 nm Maximum degradation capacity = 90% in 45 min	Tayel et al. (2018)
12	TiO2-reduced graphene oxide nanocomposites	Photodegradation activity: carbamazepine, ibuprofen, and sulfamethoxazole	Average particle size = 21 nm Maximum degradation capacity = 92% in 180 min	Lin et al. (2017b)
13	rGO/TiO_2 nanocomposites	Photodegradation activity: CBZ	Average particle size = 25 nm Surface area = 50 m^2/g Maximum degradation capacity = 99% in 90 min	Nawaz et al. (2017)

more on other bacteria such as *Salmonella enteritidis*, *Staphylococcus epidermidis*, *Salmonella typhimurium*, *Enterococcus faecalis*, *Pseudomonas aeruginosa* and *Bacillus subtilis* to provide a better perspective on the general antimicrobial ability of nanocomposites. This will reflect the growing resistance of antibiotics to various bacteria, which is becoming a serious challenge to public health worldwide.

Many factors are associated with nanomaterials' influence on anti-microbial properties and wastewater treatment, including their shape, size, functional groups, defects and orientation. Aggregated nanomaterials are found to be less effective than well-dispersed nanomaterials for both antimicrobial and wastewater treatments. Furthermore, small-sized nanoparticle-based nanocomposites are more effective for antimicrobial activities since they possess a large surface area in contact with the bacteria.

A wide variety of adsorbents have been studied to improve the adsorption performance. The three principles dye-removing mechanisms discussed are electrostatic interactions, hydrogen bonding and ion-exchange effects. The analysis shows that either modified or composite adsorbents with a high area are associated with a larger adsorption

Table 10 TiO_2-based nanocomposite's antimicrobial properties

S. no.	TiO_2-based nanocomposite	Bacteria model(s)	Findings	References
1	Titanium dioxide-decorated multi-walled carbon nanotubes nanocomposite	*Bacillus subtilis*	Average crystal size = 36 nm	Raie et al. (2018)
2	Titanium-tin oxide nanocomposite	*S. aureus, P. aeruginosa, C. albicans* and *Trichophytons*	Average diameter = 34 nm Inhibition zones, *S. aureus* = 23, *P. aeruginosa* = 21, *C. albicans* = 20 and *Trichophytons* = 20	Mahfooz-Ur-Rehman et al. (2019)
3	TiO_2/ZnO nanocomposites	*Staphylococcus aureus, Pseudomonas fluorescens, Listeria monocytogenes and Escherichia coli*	Average crystal size = 50 nm Highest inhibition zone, *Escherichia coli* = *10.73*	Azizi-Lalabadi et al. (2019)
4	Silver-titanium dioxide nanocomposite	*Escherichia coli*	Average particle size = 4.9 nm BET surface area = 151 m^2/g 90% *E. Coli* kill in 240-min	Yang et al. (2014)
5	Graphene oxide/TiO_2 nanocomposites	*Staphylococcus aureus* and *Enterococcus faecalis*	Average particle size = 150 nm	Stan et al. (2018)

capacity. Furthermore, constraints such as initial dye concentration, temperature, the dose of adsorbent and pH are critical factors that show significant effects on dye adsorption. In this review, frequently used isotherms, kinetic models and thermodynamic models are also examined to describe the adsorption process. A pseudo-second-order model and Langmuir isotherm were found to be best fitted in the experimental data in the majority of cases. From thermodynamic studies, it is revealed that the process of adsorption is spontaneous and endothermic in nature. Most of the studies in the literature focused on color removal only. Different constituents from dye effluents should be focused on in future studies rather than focusing only on color removal. The area of interest that can be investigated is synthesizing various adsorbents through eco-friendly routes.

Although the adsorption process is well-established and has been widely used for many decades, further exciting prospects for developing innovative and renewable green materials with higher selectivity and stability at a lower cost need attention. In the next few years, it will be important to face the challenges emerging from the translation of lab adsorption research into pilot and industrial processes, such as economic constraints, comprehensive regeneration and the over-utilization of chemical agents.

Conclusion

This paper explores the existing nanocomposites used to extract heavy metal ions and dyes from wastewater as effective adsorbents. This article addressed recent developments in nanomaterials as economical and environmentally sustainable water purification adsorbents. This review highlights five commonly used nanomaterials/nanoparticles that are used in most existing nanocomposites. In this review, we concluded that TiO_2-based nanocomposites have been used for photodegradation activity by most of the researchers in the literature. Silver-based nanocomposites are mostly used for antimicrobial activity. Silver and GO-based nanocomposites were used for the removal of green dye, anionic dye and Cu(II). Copper-based nanocomposites are mostly used for adsorption and photodegradation activity. Zinc oxide nanocomposites are used for adsorption, antimicrobial and photodegradation activity. Finally, we concluded that GO also greatly contributes to the improvement of other materials' efficiency. Further, much needs to be done to control the two-dimensional GO sheets for advanced technologies in the future. There are many challenges and obstacles associated with handling wastewater, and many precautions are required to prevent environmental and health problems. Therefore, new modern wastewater treatment equipment should be versatile, low-cost and commercially effective.

Acknowledgement We are thankful to Dr. Tariq M. Khan for drawing all the color figures for the manuscript.

Declarations

Conflict of interest The authors declare that they have no conflict of interest.

References

Abou El-Nour KMM, Eftaiha A, Al-Warthan A, Ammar RAA (2010) Synthesis and applications of silver nanoparticles. Arab J Chem 3:135–140

Abubakar H (2020) Preparation and characterization of zinc oxide/clay minerals nanocomposites as adsorbent for removal of Cu (II) and Pb (II) ions Citation Additional Metadata. 5–7

Adams LK, Lyon DY, Alvarez PJJ (2006) Comparative eco-toxicity of nanoscale TiO_2, SiO_2, and ZnO water suspensions. Water Res 40:3527–3532

Ahmad M, Ahmed E, Hong ZL, Khalid NR, Ahmed W, Elhissi A (2013a) Graphene–Ag/ZnO nanocomposites as high performance photocatalysts under visible light irradiation. J Alloys Compd 577:717–727. https://doi.org/10.1016/j.jallcom.2013.06.137

Ahmad M, Ahmed E, Hong ZL, Xu JF, Khalid NR, Elhissi A, Ahmed W (2013b) A facile one-step approach to synthesizing ZnO/graphene composites for enhanced degradation of methylene blue under visible light. Appl Surf Sci 274:273–281. https://doi.org/10.1016/j.apsusc.2013.03.035

Ahmad R (2019) Polyaniline/ZnO nanocomposite: a novel adsorbent for the removal of Cr (VI) from aqueous solution. Adv Compos Mater Dev 1–22

Akyildiz HI, Michielsen S (2013) Improving water solubility of poly(acrylic acid-co-styrene) copolymers by adding styrene sulfonic acid as a termonomer. J Appl Polym Sci 129:2208–2215. https://doi.org/10.1002/app.38933

Al-Thabaiti SA, Al-Nowaiser FM, Obaid AY, Al-Youbi AO, Khan Z (2008) Formation and characterization of surfactant stabilized silver nanoparticles: a kinetic study. Colloids Surfaces B Biointerfaces 67:230–237

Ali I (2012) New generation adsorbents for water treatment. Chem Rev 112:5073–5091. https://doi.org/10.1021/cr300133d

Alsharaeh E, Alazzam S, Ahmed F, Arshi N, Al-Hindawi M, Sing GK (2017) Green synthesis of silver nanoparticles and their reduced graphene oxide nanocomposites as antibacterial agents: a bio-inspired approach. Acta Metall Sin English Lett 30:45–52. https://doi.org/10.1007/s40195-016-0485-z

Alswata AA, Bin AM, Al-Hada NM, Kamari HM, Bin HMZ, Ibrahim NA (2017) Preparation of zeolite/zinc oxide nanocomposites for toxic metals removal from water. Results Phys 7:723–731. https://doi.org/10.1016/j.rinp.2017.01.036

Amalraj Appavoo I, Hu J, Huang Y, Li SFY, Ong SL (2014) Response surface modeling of Carbamazepine (CBZ) removal by Graphene-P25 nanocomposites/UVA process using central composite design. Water Res 57:270–279. https://doi.org/10.1016/j.watres.2014.03.007

Amini M, Rahimpour A, Jahanshahi M (2016) Forward osmosis application of modified TiO_2-polyamide thin film nanocomposite membranes. Desalin Water Treat 57:14013–14023. https://doi.org/10.1080/19443994.2015.1065441

Anandan S, Narasinga RT, Sathish M, Rangappa D, Honma I, Miyauchi M (2013) Superhydrophilic graphene-loaded TiO_2 thin film for self-cleaning applications. ACS Appl Mater Interfaces 5:207–212. https://doi.org/10.1021/am302557z

Anjaneyulu RB, Mohan BS, Naidu GP, Muralikrishna R (2018) Visible light enhanced photocatalytic degradation of methylene blue by ternary nanocomposite, MoO_3/Fe_2O_3/rGO. J Asian Ceram Soc 6:183–195. https://doi.org/10.1080/21870764.2018.1479011

Annamalai T, Joel J, Ayyar G, Prince AAM (2018) Chitosan-zinc oxide with MMT K10 superadsorbent nanocomposites: synthesis, characterization and its antibacterial activity. Int J Green Second Metab Plant Manilkara Hexandra 7:715–724. https://doi.org/10.24214/IJGHC/GC/7/4

Archana S, Kumar KY, Jayanna BK, Olivera S, Anand A, Prashanth MK, Muralidhara HB (2018) Versatile Graphene oxide decorated by star shaped Zinc oxide nanocomposites with superior adsorption capacity and antimicrobial activity. J Sci Adv Mater Devices 3:167–174. https://doi.org/10.1016/j.jsamd.2018.02.002

Attia AJ, Kadhim SH, Hussein FH (2007) Photocatalytic degradation of textile dyeing wastewater using titanium dioxide and zinc oxide. E-J Chem 5:219–223

Azeredo de HMC (2009) Nanocomposites for food packaging applications. Food Res Int 42:1240–1253. https://doi.org/10.1016/j.foodres.2009.03.019

Azizi-Lalabadi M, Ehsani A, Divband B, Alizadeh-Sani M (2019) Antimicrobial activity of Titanium dioxide and Zinc oxide nanoparticles supported in 4A zeolite and evaluation the morphological characteristic. Sci Rep 9:17439. https://doi.org/10.1038/s41598-019-54025-0

Baek Y-W, An Y-J (2011) Microbial toxicity of metal oxide nanoparticles (CuO, NiO, ZnO, and Sb_2O_3) to *Escherichia coli*, *Bacillus subtilis*, and *Streptococcus aureus*. Sci Total Environ 409:1603–1608

Bagavathy MS, Perachiselvi M, Feiona TA, Krishnaveni P, Pushpalaksmi E, Swetha V, Britto SJ, Annadurai G (2019) Adsorption and antibacterial studies using encapsulated chitosan/ZnO nanocomposite. Res J LIfe Sci Bioinform Pharm Chem Sci 5:735–755. https://doi.org/10.26479/2019.0501.62

Balandin AA, Ghosh S, Bao W, Calizo I, Teweldebrhan D, Miao F, Lau CN (2008) Superior thermal conductivity of single-layer graphene. Nano Lett 8:902–907. https://doi.org/10.1021/nl0731872

Bao Q, Zhang D, Qi P (2011) Synthesis and characterization of silver nanoparticle and graphene oxide nanosheet composites as a bactericidal agent for water disinfection. J Colloid Interface Sci 360:463–470. https://doi.org/10.1016/j.jcis.2011.05.009

Basu S, Bhattacharyya P (2012) Recent developments on graphene and graphene oxide based solid state gas sensors. Sensors Actuators B Chem 173:1–21

Bhavyasree PG, Xavier TS (2020) Green synthesis of copper oxide/carbon nanocomposites using the leaf extract of *Adhatoda vasica* Nees, their characterization and antimicrobial activity. Heliyon 6:e03323. https://doi.org/10.1016/j.heliyon.2020.e03323

Bitton G (2005) Wastewater microbiology. Wiley-Liss

Bolotin KI, Sikes KJ, Jiang Z, Klima M, Fudenberg G, Hone J, Kim P, Stormer HL (2008) Ultrahigh electron mobility in suspended graphene

Borgohain K, Mahamuni S (2002) Formation of single-phase CuO quantum particles. J Mater Res 17:1220–1223. https://doi.org/10.1557/jmr.2002.0180

Botsa SM, Basavaiah K (2018) Removal of Nitrophenols from wastewater by monoclinic CuO/RGO nanocomposite. Nanotechnol Environ Eng 4:1. https://doi.org/10.1007/s41204-018-0045-z

Bouazizi A, Breida M, Achiou B, Ouammou M, Calvo JI, Aaddane A, Younssi SA (2017) Removal of dyes by a new nano-TiO_2 ultrafiltration membrane deposited on low-cost support prepared from natural Moroccan bentonite. Appl Clay Sci 149:127–135. https://doi.org/10.1016/j.clay.2017.08.019

Bouazizi N, Vieillard J, Thebault P, Desriac F, Clamens T, Bargougui R, Couvrat N, Thoumire O, Brun N, Ladam G, Morin S, Mofaddel N, Lesouhaitier O, Azzouz A, Le Derf F (2018) Silver nanoparticle embedded copper oxide as an efficient core–shell for the catalytic reduction of 4-nitrophenol and antibacterial activity improvement. Dalt Trans 47:9143–9155. https://doi.org/10.1039/C8DT02154F

Bukman L, Fernandes-Machado NRC, Caetano W, Tessaro AL, Hioka N (2017) Treatment of wastewater contaminated with ionic dyes: liquid-liquid extraction induced by reversed micelle followed by photodegradation. Sep Purif Technol 189:162–169. https://doi.org/10.1016/j.seppur.2017.08.004

Chandra V, Park J, Chun Y, Lee JW, Hwang I-C, Kim KS (2010) Water-dispersible magnetite-reduced graphene oxide composites for arsenic removal. ACS Nano 4:3979–3986. https://doi.org/10.1021/nn1008897

Chang Y-N, Ou X-M, Zeng G-M, Gong J-L, Deng C-H, Jiang Y, Liang J, Yuan G-Q, Liu H-Y, He X (2015) Synthesis of magnetic graphene oxide-TiO_2 and their antibacterial properties under solar irradiation. Appl Surf Sci 343:1–10. https://doi.org/10.1016/j.apsusc.2015.03.082

Chang Y, Zeng HC (2004) Controlled synthesis and self-assembly of single-crystalline CuO nanorods and nanoribbons. Cryst Growth Des 4:397–402. https://doi.org/10.1021/cg034127m

Chella S, Kollu P, Komarala EVPR, Doshi S, Saranya M, Felix S, Ramachandran R, Saravanan P, Koneru VL, Venugopal V, Jeong SK, Nirmala Grace A (2015) Solvothermal synthesis of $MnFe_2O_4$-graphene composite—investigation of its adsorption and antimicrobial properties. Appl Surf Sci 327:27–36. https://doi.org/10.1016/j.apsusc.2014.11.096

Cheremisinoff NP (2002) Handbook of water and wastewater treatment technologies. Butterworth-Heinemann

Chou T-W, Gao L, Thostenson ET, Zhang Z, Byun J-H (2010) An assessment of the science and technology of carbon nanotube-based fibers and composites. Compos Sci Technol 70:1–19. https://doi.org/10.1016/j.compscitech.2009.10.004

Chowdhury S, Rodriguez MJ, Sadiq R (2011) Disinfection byproducts in Canadian provinces: associated cancer risks and medical expenses. J Hazard Mater 187:574–584

Christian P, Von der Kammer F, Baalousha M, Hofmann T (2008) Nanoparticles: structure, properties, preparation and behaviour in environmental media. Ecotoxicology 17:326–343. https://doi.org/10.1007/s10646-008-0213-1

Cioffi N, Ditaranto N, Torsi L, Picca RA, De Giglio E, Sabbatini L, Novello L, Tantillo G, Bleve-Zacheo T, Zambonin PG (2005) Synthesis, analytical characterization and bioactivity of Ag and Cu nanoparticles embedded in poly-vinyl-methyl-ketone films. Anal Bioanal Chem 382:1912–1918

da Silva TH, Ribeiro AO, Nassar EJ, Trujillano R, Rives V, Vicente MA, de Faria EH, Ciuffi KJ (2019) Kaolinite/TiO_2/cobalt(II) tetracarboxymetallophthalocyanine nanocomposites as heterogeneous photocatalysts for decomposition of organic pollutants trimethoprim, caffeine and prometryn. J Braz Chem Soc 30:2610–2623. https://doi.org/10.21577/0103-5053.20190178

Daus B, Wennrich R, Weiss H (2004) Sorption materials for arsenic removal from water: a comparative study. Water Res 38:2948–2954

de Mendonça VR, Mourão HAJL, Malagutti AR, Ribeiro C (2019) The role of the relative dye/photocatalyst concentration in TiO_2 assisted photodegradation process. Photochem Photobiol 90:66–72. https://doi.org/10.1111/php.12175

Deng C-H, Gong J-L, Zeng G-M, Niu C-G, Niu Q-Y, Zhang W, Liu H-Y (2014) Inactivation performance and mechanism of *Escherichia coli* in aqueous system exposed to iron oxide loaded graphene nanocomposites. J Hazard Mater 276:66–76. https://doi.org/10.1016/j.jhazmat.2014.05.011

Dhand V, Rhee KY, Jung HJKDH (2013) A comprehensive review of graphene nanocomposites: research status and trends. J Nanomater 2013:1–14

Domènech B, Muñoz M, Muraviev D, Macanás J (2013) Polymer-silver nanocomposites as antibacterial materials, pp. 630–640

Dubey SP, Nguyen TTM, Kwon Y-N, Lee C (2015) Synthesis and characterization of metal-doped reduced graphene oxide composites, and their application in removal of *Escherichia coli*, arsenic and 4-nitrophenol. J Ind Eng Chem 29:282–288. https://doi.org/10.1016/j.jiec.2015.04.008

Ebina T, Minja RJA, Wakui Y, Chatterjee A, Onodera Y, Stucky DG (2015) Synthesis and arsenic adsorption capability of smectite-titanium oxide nanocomposite of tunable pore size. Clay Sci. https://doi.org/10.1017/CBO9781107415324.004

Egirani D, Latif MT, Wessey N, Poyi NR, Acharjee S (2019) Synthesis and characterization of kaolinite coated with copper oxide and its effect on the removal of aqueous Lead(II) ions. Appl Water Sci 9:109. https://doi.org/10.1007/s13201-019-0989-6

El-Liethy MA, Elwakeel KZ, Ahmed MS (2018) Comparison study of Ag(I) and Au(III) loaded on magnetic thiourea-formaldehyde as disinfectants for water pathogenic microorganism's deactivation. J Environ Chem Eng 6:4380–4390. https://doi.org/10.1016/j.jece.2018.06.028

El-Tawil RS, El-Wakeel ST, Abdel-Ghany AE, Abuzeid HAM, Selim KA, Hashem AM (2019) Silver/quartz nanocomposite as an adsorbent for removal of mercury (II) ions from aqueous solutions. Heliyon 5:e02415–e02415. https://doi.org/10.1016/j.heliyon.2019.e02415

El Essawy NA, Ali SM, Farag HA, Konsowa AH, Elnouby M, Hamad HA (2017) Green synthesis of graphene from recycled PET bottle wastes for use in the adsorption of dyes in aqueous solution. Ecotoxicol Environ Saf 145:57–68. https://doi.org/10.1016/j.ecoenv.2017.07.014

El Saeed AM, El-Fattah MA, Azzam AM (2015) Synthesis of ZnO nanoparticles and studying its influence on the antimicrobial, anticorrosion and mechanical behavior of polyurethane composite for surface coating. Dye Pigment 121:282–289

Ellis TG (2004) Chemistry of wastewater. Encyclopedia of life support system (EOLSS)

Elwakeel KZ, Al-Bogami AS, Guibal E (2021) 2-Mercaptobenzimidazole derivative of chitosan for silver sorption—contribution of magnetite incorporation and sonication effects on enhanced metal recovery. Chem Eng J 403:126265. https://doi.org/10.1016/j.cej.2020.126265

Elwakeel KZ, El-Liethy MA, Ahmed MS, Ezzat SM, Kamel MM (2018) Facile synthesis of magnetic disinfectant immobilized with silver ions for water pathogenic microorganism's deactivation. Environ Sci Pollut Res 25:22797–22809. https://doi.org/10.1007/s11356-018-2071-6

Elwakeel KZ, Elgarahy AM, Guibal E (2020a) A biogenic tunable sorbent produced from upcycling of aquatic biota-based materials functionalized with methylene blue dye for the removal of chromium (VI) ions. J Environ Chem Eng. https://doi.org/10.1016/j.jece.2020.104767

Elwakeel KZ, Elgarahy AM, Khan ZA, Almughamisi MS, Al-Bogami AS (2020b) Perspectives regarding metal/mineral-incorporating materials for water purification: with special focus on Cr (VI) removal. Mater Adv 1:1546–1574. https://doi.org/10.1039/d0ma00153h

Elwakeel KZ, Shahat A, Al-Bogami AS, Wijesiri B, Goonetilleke A (2020c) The synergistic effect of ultrasound power and magnetite incorporation on the sorption/desorption behavior of Cr(VI) and As(V) oxoanions in an aqueous system. J Colloid Interface Sci 569:76–88. https://doi.org/10.1016/j.jcis.2020.02.067

Elwakeel KZ, Shahat A, Khan ZA, Alshitari W, Guibal E (2020d) Magnetic metal oxide-organic framework material for ultrasonic-assisted sorption of titan yellow and rose bengal from aqueous solutions. Chem Eng J 392:123635. https://doi.org/10.1016/j.cej.2019.123635

Esmailzadeh H, Sangpour P, Shahraz F, Hejazi J, Khaksar R (2016) Effect of nanocomposite packaging containing ZnO on growth of *Bacillus subtilis* and *Enterobacter aerogenes*. Mater Sci Eng C 58:1058–1063

Evangelou VP (1998) Environmental soil and water chemistry: principles and applications. Wiley, New York

Ezzatahmadi N, Ayoko GA, Millar GJ, Speight R, Yan C, Li J, Li S, Zhu J, Xi Y (2017) Clay-supported nanoscale zero-valent iron composite materials for the remediation of contaminated aqueous solutions: a review. Chem Eng J 312:336–350. https://doi.org/10.1016/j.cej.2016.11.154

Fahmy A, Eisa W, Yosef M, Hassan A (2016) Ultra-thin films of poly(acrylic acid)/silver nanocomposite coatings for

antimicrobial applications. J Spectrosc 2016:1–11. https://doi.org/10.1155/2016/7489536
Fan G, Wang Y, Fang G, Zhu X, Zhou D (2016) Review of chemical and electrokinetic remediation of PCBs contaminated soils and sediments. Environ Sci Process Impacts 18:1140–1156. https://doi.org/10.1039/C6EM00320F
Faust SD, Aly OM (1983) Chemistry of water treatment. Butterworth, Stoneham
Fu G, Vary PS, Lin C-T (2005) Anatase TiO_2 nanocomposites for antimicrobial coatings. J Phys Chem B 109:8889–8898. https://doi.org/10.1021/jp0502196
Fuqua GW (2010) A comparative review of water disinfection methods appropriate for developing countries and their efficacy, cost-efficiency, and usability
Gandhi MR, Vasudevan S, Shibayama A, Yamada M (2019) Graphene and graphene-based composites: a rising star in water purification—a comprehensive overview. ChemistrySelect 1:4358–4385. https://doi.org/10.1002/slct.201600693
Ganguly S, Das P, Bose M, Das TK, Mondal S, Das AK, Das NC (2017) Sonochemical green reduction to prepare Ag nanoparticles decorated graphene sheets for catalytic performance and antibacterial application. Ultrason Sonochem 39:577–588. https://doi.org/10.1016/j.ultsonch.2017.05.005
Gayathri S, Kottaisamy M, Ramakrishnan V (2015) Facile microwave-assisted synthesis of titanium dioxide decorated graphene nanocomposite for photodegradation of organic dyes. AIP Adv. https://doi.org/10.1063/1.4938544
Ghorbi E, Namavar M, Rashedi V, Farhadinejad S, Jahromi SP, Zareian M (2019) Influence of nano-copper oxide concentration on bactericidal properties of silver-copper oxide nanocomposite
Giannelis EP (1996) Polymer layered silicate nanocomposites. Adv Mater 8:29–35. https://doi.org/10.1002/adma.19960080104
Gunti S (2017) Enhanced visible light photocatalytic remediation of organics in water using zinc oxide and titanium oxide nanostructures
Gurunathan S, Han JW, Dayem AA, Eppakayala V, Park M-R, Kwon D-N, Kim J-H (2013) Antibacterial activity of dithiothreitol reduced graphene oxide. J Ind Eng Chem 19:1280–1288
Hassan H, Salama A, El-ziaty AK, El-Sakhawy M (2019) New chitosan/silica/zinc oxide nanocomposite as adsorbent for dye removal. Int J Biol Macromol 131:520–526. https://doi.org/10.1016/j.ijbiomac.2019.03.087
He D, Chen Y, Situ Y, Zhong L, Huang H (2017) Synthesis of ternary g-C_3N_4/Ag/γ-FeOOH photocatalyst: an integrated heterogeneous Fenton-like system for effectively degradation of azo dye methyl orange under visible light. Appl Surf Sci 425:862–872. https://doi.org/10.1016/j.apsusc.2017.06.124
Hillie T, Hlophe M (2007) Nanotechnology and the challenge of clean water. Nat Nanotechnol 2:663
Hosseini SA (2016) Graphene oxide/zinc oxide nanocomposite: a superior adsorbent for removal of methylene blue-statistical analysis by response surface methodology (RSM). S Afr J Chem 69:105–112. https://doi.org/10.17159/0379-4350/2016/v69a13
Hsu K-C, Chen D-H (2014) Green synthesis and synergistic catalytic effect of Ag/reduced graphene oxide nanocomposite. Nanoscale Res Lett 9:484. https://doi.org/10.1186/1556-276X-9-484
Huang L, Yang H, Zhang Y, Xiao W (2016) Study on synthesis and antibacterial properties of Ag NPs/GO nanocomposites. J Nanomater 2016:5685967. https://doi.org/10.1155/2016/5685967
Hussain N, Gogoi A, Sarma RK, Sharma P, Barras A, Boukherroub R, Saikia R, Sengupta P, Das MR (2014) Reduced graphene oxide nanosheets decorated with Au nanoparticles as an effective bactericide: investigation of biocompatibility and leakage of sugars and proteins. ChemPlusChem 79:1774–1784. https://doi.org/10.1002/cplu.201402240
Inglezakis VJ, Kurbanova A, Molkenova A, Zorpas AA, Atabaev TS (2020) Magnetic Fe_3O_4–Ag0 nanocomposites for effective mercury removal from water. Sustain 12
Janas D, Liszka B (2018) Copper matrix nanocomposites based on carbon nanotubes or graphene. Mater Chem Front 2:22–35. https://doi.org/10.1039/C7QM00316A
Jaworski S, Wierzbicki M, Sawosz E, Jung A, Gielerak G, Biernat J, Jaremek H, Łojkowski W, Woźniak B, Wojnarowicz J, Stobiński L, Małolepszy A, Mazurkiewicz-Pawlicka M, Łojkowski M, Kurantowicz N, Chwalibog A (2018) Graphene oxide-based nanocomposites decorated with silver nanoparticles as an antibacterial agent. Nanoscale Res Lett 13:116. https://doi.org/10.1186/s11671-018-2533-2
Jeyapragasam T (2016) Synthesis of silver-graphene oxide nanocomposite for removal of anionic dye by adsorption. Mater Today Proc 3:2146–2154. https://doi.org/10.1016/j.matpr.2016.04.120
Jun-e Q, Zhou S, Wang H, Cao Z, Hongfang L (2017) The application of an activated carbon supported Cu-Ce/Ac oxide anode on the electrocatalytic degradation of phenol. Int J Electrochem Sci 12:9640–9651. https://doi.org/10.20964/2017.10.09
Karim S, Mumtaz A, Hasanain K, Liu J, Duan J (2008) Synthesis and magnetic characterization of nickel ferrite nanoparticles prepared by co-precipitation route. J Magn Magn Mater. https://doi.org/10.1016/j.jmmm.2008.11.098
Karimi L (2017) Combination of mesoporous titanium dioxide with MoS_2 nanosheets for high photocatalytic activity. Polish J Chem Technol 19:56–60. https://doi.org/10.1515/pjct-2017-0028
Khorrami S, Abdollahi Z, Eshaghi G, Khosravi A, Bidram E, Zarrabi A (2019) An improved method for fabrication of Ag-GO nanocomposite with controlled anti-cancer and anti-bacterial behavior. A comparative study. Sci Rep 9:9167. https://doi.org/10.1038/s41598-019-45332-7
Khosravian P, Ghashang M, Ghayoor H (2017) Effective removal of penicillin from aqueous solution using zinc oxide/natural-zeolite composite nano-powders prepared via ball milling technique. Recent Pat Nanotechnol 11:2–3. https://doi.org/10.2174/1872210511666170105141550
Kim H, Kang S-O, Park S, Park HS (2015) Adsorption isotherms and kinetics of cationic and anionic dyes on three-dimensional reduced graphene oxide macrostructure. J Ind Eng Chem 21:1191–1196
Klarich KL, Pflug NC, DeWald EM, Hladik ML, Kolpin DW, Cwiertny DM, LeFevre GH (2017) Occurrence of neonicotinoid insecticides in finished drinking water and fate during drinking water treatment. Environ Sci Technol Lett 4:168–173. https://doi.org/10.1021/acs.estlett.7b00081
Konkena B, Vasudevan S (2012) Covalently linked, water-dispersible, cyclodextrin: reduced-graphene oxide sheets. Langmuir 28:12432–12437. https://doi.org/10.1021/la3020783
Koo H, Lee H-J, Go H-A, Lee Y, Bae T, Kim J, Choi W (2011) Graphene-based multifunctional iron oxide nanosheets with tunable properties. Chemistry 17:1214–1219. https://doi.org/10.1002/chem.201002252
Kravchenko GV, Domoroshchina EN, Kuzmicheva GM, Gaynanova AA, Amarantov SV, Pirutko LV, Tsybinsky AM, Sadovskaya NV, Kopylova EV (2016) Zeolite-titanium dioxide nanocomposites: preparation, characterization, and adsorption properties. Nanotechnologies Russ 11:579–592. https://doi.org/10.1134/S1995078016050098
Kumari S, Sharma P, Yadav S, Kumar J, Vij A, Rawat P, Kumar S, Sinha C, Bhattacharya J, Srivastava CM, Majumder S (2020) A novel synthesis of the graphene oxide-silver (GO-Ag) nanocomposite for unique physiochemical applications. ACS Omega 5:5041–5047. https://doi.org/10.1021/acsomega.9b03976
Lakkaboyana SK, Khantong S, Asmel NK, Yuzir A, Wan Yaacob WZ (2019) Synthesis of copper oxide nanowires-activated carbon

(AC@CuO-NWs) and applied for removal methylene blue from aqueous solution: kinetics, isotherms, and thermodynamics. J Inorg Organomet Polym Mater 29:1658–1668. https://doi.org/10.1007/s10904-019-01128-w

Lee C, Wei X, Kysar JW, Hone J (2008) Measurement of the elastic properties and intrinsic strength of monolayer graphene. Science (80-) 321:385

Lekota MW, Dimpe KM, Nomngongo PN (2019) MgO-ZnO/carbon nanofiber nanocomposite as an adsorbent for ultrasound-assisted dispersive solid-phase microextraction of carbamazepine from wastewater prior to high-performance liquid chromatographic detection. J Anal Sci Technol 10:1–12. https://doi.org/10.1186/s40543-019-0185-1

Li D, Müller MB, Gilje S, Kaner RB, Wallace GG (2008) Processable aqueous dispersions of graphene nanosheets. Nat Nanotechnol 3:101–105

Li H, Liu S, Zhao J, Feng N (2016) Removal of reactive dyes from wastewater assisted with kaolin clay by magnesium hydroxide coagulation process. Colloids Surfaces A Physicochem Eng Asp 494:222–227. https://doi.org/10.1016/j.colsurfa.2016.01.048

Li J, Guo S, Zhai Y, Wang E (2009) Nafion-Graphene nanocomposite film as enhanced sensing platform for ultrasensitive determination of cadmium. Electrochem commun 11:1085–1088. https://doi.org/10.1016/j.elecom.2009.03.025

Li Z, Liu D, Huang W, Wei X, Huang W (2020) Biochar supported CuO composites used as an efficient peroxymonosulfate activator for highly saline organic wastewater treatment. Sci Total Environ 721:137764. https://doi.org/10.1016/j.scitotenv.2020.137764

Lin L, Wang H, Jiang W, Mkaouar AR, Xu P (2017a) Comparison study on photocatalytic oxidation of pharmaceuticals by TiO_2-Fe and TiO_2-reduced graphene oxide nanocomposites immobilized on optical fibers. J Hazard Mater 333:162–168. https://doi.org/10.1016/j.jhazmat.2017.02.044

Lin L, Wang H, Xu P (2017b) Immobilized TiO2-reduced graphene oxide nanocomposites on optical fibers as high performance photocatalysts for degradation of pharmaceuticals. Chem Eng J 310:389–398. https://doi.org/10.1016/j.cej.2016.04.024

Liu G, Li L, Xu D, Huang X, Xu X, Zheng S, Zhang Y, Lin H (2017) Metal-organic framework preparation using magnetic graphene oxide–β-cyclodextrin for neonicotinoid pesticide adsorption and removal. Carbohydr Polym 175:584–591. https://doi.org/10.1016/j.carbpol.2017.06.074

Liu J, Shao J, Wang Y, Li J, Liu H, Wang A, Hui A, Chen S (2019) Antimicrobial activity of zinc oxide-graphene quantum dot nanocomposites: enhanced adsorption on bacterial cells by cationic capping polymers. ACS Sustain Chem Eng 7:16264–16273. https://doi.org/10.1021/acssuschemeng.9b03292

Liu M, Chen C, Hu J, Wu X, Wang X (2011) Synthesis of magnetite/graphene oxide composite and application for cobalt(II) removal. J Phys Chem C 115:25234–25240. https://doi.org/10.1021/jp208575m

Liu M, Wen T, Wu X, Chen C, Hu J, Li J, Wang X (2013) Synthesis of porous Fe_3O_4 hollow microspheres/graphene oxide composite for Cr(vi) removal. Dalt Trans 42:14710–14717. https://doi.org/10.1039/C3DT50955A

Luo X, Wang C, Luo S, Dong R, Tu X, Zeng G (2012) Adsorption of As (III) and As (V) from water using magnetite Fe_3O_4-reduced graphite oxide–MnO2 nanocomposites. Chem Eng J 187:45–52. https://doi.org/10.1016/j.cej.2012.01.073

Madaeni SS, Zinadini S, Vatanpour V (2011) A new approach to improve antifouling property of PVDF membrane using in situ polymerization of PAA functionalized TiO_2 nanoparticles. J Memb Sci 380:155–162. https://doi.org/10.1016/j.memsci.2011.07.006

Mahfooz-Ur-Rehman M, Rehman W, Waseem M, Shah BA, Shakeel M, Haq S, Zaman U, Bibi I, Khan HD (2019) Fabrication of titanium-tin oxide nanocomposite with enhanced adsorption and antimicrobial applications. J Chem Eng Data 64:2436–2444. https://doi.org/10.1021/acs.jced.8b01243

Majdalawi M, Krishan M (2019) Adsorption of cationic and anionic organic dyes on SiO_2/CuO composite. Desalin Water Treat. https://doi.org/10.5004/dwt.2019.24706

Manias E (2007) Nanocomposites: stiffer by design. Nat Mater 6:9–11. https://doi.org/10.1038/nmat1812

Mauter MS, Elimelech M (2008) Environmental applications of carbon-based nanomaterials. Environ Sci Technol 42:5843–5859. https://doi.org/10.1021/es8006904

Moghayedi M, Goharshadi EK, Ghazvini K, Ahmadzadeh H, Ranjbaran L, Masoudi R, Ludwig R (2017) Kinetics and mechanism of antibacterial activity and cytotoxicity of Ag-RGO nanocomposite. Colloids Surf B Biointerfaces 159:366–374. https://doi.org/10.1016/j.colsurfb.2017.08.001

Mokhtari P, Ghaedi M, Dashtian K, Rahimi MR, Purkait MK (2016) Removal of methyl orange by copper sulfide nanoparticles loaded activated carbon: kinetic and isotherm investigation. J Mol Liq 219:299–305. https://doi.org/10.1016/j.molliq.2016.03.022

Motshekga SC, Ray SS, Onyango MS, Momba MNB (2015) Preparation and antibacterial activity of chitosan-based nanocomposites containing bentonite-supported silver and zinc oxide nanoparticles for water disinfection. Appl Clay Sci 114:330–339

Mousa M (2013) Wastewater disinfection by synthesized copper oxide nanoparticles stabilized with surfactant

Muravyov MI, Fomchenko NV, Usoltsev AV, Vasilyev EA, Kondrateva TF (2012) Leaching of copper and zinc from copper converter slag flotation tailings using H2SO4 and biologically generated $Fe_2(SO_4)_3$. Hydrometallurgy 119–120:40–46. https://doi.org/10.1016/j.hydromet.2012.03.001

Naseem T, Durrani T (2021) The role of some important metal oxide nanoparticles for wastewater and antibacterial applications: a review. Environ Chem Ecotoxicol. https://doi.org/10.1016/j.enceco.2020.12.001

Naseem T, Abdin Z, Waseem M, Hafeez M, Din SU, Haq S, Rehman M (2020) Reduced graphene oxide/zinc oxide nanocomposite: from synthesis to its application for wastewater purification and antibacterial activity. J Inorg Organomet Polym Mater. https://doi.org/10.1007/s10904-020-01529-2

Nawaz M, Miran W, Jang J, Lee DS (2017) One-step hydrothermal synthesis of porous 3D reduced graphene oxide/TiO_2 aerogel for carbamazepine photodegradation in aqueous solution. Appl Catal B Environ 203:85–95. https://doi.org/10.1016/j.apcatb.2016.10.007

Nemati M, Saboori R, Sabbaghi S (2019) Hydrogen sulfide removal using various metal oxide nanocomposite from drilling fluid: optimization, kinetic and adsorption isotherms

Ni Z, Wang Z, Sun L, Li B, Zhao Y (2014) Synthesis of poly acrylic acid modified silver nanoparticles and their antimicrobial activities. Mater Sci Eng C 41:249–254. https://doi.org/10.1016/j.msec.2014.04.059

Nishio J, Tokumura M, Znad HT, Kawase Y (2006) Photocatalytic decolorization of azo-dye with zinc oxide powder in an external UV light irradiation slurry photoreactor. J Hazard Mater 138:106–115

Nourmohammadi A, Rahighi R, Akhavan O, Moshfegh A (2014) Graphene oxide sheets involved in vertically aligned zinc oxide nanowires for visible light photoinactivation of bacteria. J Alloys Compd 612:380–385. https://doi.org/10.1016/j.jallcom.2014.05.195

Pandian L, Rajasekaran R, Govindan P (2018) Synthesis, characterization and application of Cu doped ZnO nanocatalyst for photocatalytic ozonation of textile dye and study of its

reusability. Mater Res Express 5:115505. https://doi.org/10.1088/2053-1591/aadcdf

Pang S, He Y, Zhong R, Guo Z, He P, Zhou C, Xue B, Wen X, Li H (2019) Multifunctional ZnO/TiO_2 nanoarray composite coating with antibacterial activity, cytocompatibility and piezoelectricity. Ceram Int 45:12663–12671. https://doi.org/10.1016/j.ceramint.2019.03.076

Pant B, Saud PS, Park M, Park S-J, Kim H-Y (2016) General one-pot strategy to prepare Ag–TiO_2 decorated reduced graphene oxide nanocomposites for chemical and biological disinfectant. J Alloys Compd 671:51–59. https://doi.org/10.1016/j.jallcom.2016.02.067

Pare B, Singh P, Jonnalgadda SP (2009) Artificial light assisted photocatalytic degradation of lissamine fast yellow dye in ZnO suspension in a slurry batch reactor. Indian J Chem 1364–1369

Pelgrift RY, Friedman AJ (2013) Nanotechnology as a therapeutic tool to combat microbial resistance. Adv Drug Deliv Rev 65:1803–1815. https://doi.org/10.1016/j.addr.2013.07.011

Penlidis A Water Soluble Polymers Edited by

Petica A, Florea A, Gaidau C, Balan D, Anicai L (2017) Synthesis and characterization of silver-titania nanocomposites prepared by electrochemical method with enhanced photocatalytic characteristics, antifungal and antimicrobial activity. J Mater Res Technol

Qin YL, Zhao WW, Sun Z, Liu XY, Shi GL, Liu ZY, Ni DR, Ma ZY (2019) Photocatalytic and adsorption property of ZnS–TiO_2/RGO ternary composites for methylene blue degradation. Adsorpt Sci Technol 37:764–776. https://doi.org/10.1177/0263617418810932

Qu X, Alvarez PJJ, Li Q (2013) Applications of nanotechnology in water and wastewater treatment. Water Res 47:3931–3946. https://doi.org/10.1016/j.watres.2012.09.058

Rachna US (2020) Photocatalytic degradation of toxic phenols using zinc oxide doped. ICNN 2020 Int Conf Nanosci Nanotechnol 14:2020

Rahdar A, Aliahmad M, Azizi Y, Keikha N, Moudi M, Keshavarzi F (2017) CuO-NiO nano composites: synthesis, characterization, and cytotoxicity evaluation. Nanomedicine Res J 2:78–86. https://doi.org/10.22034/nmrj.2017.56956.1057

Raie DS, Mhatre E, El-Desouki DS, Labena A, El-Ghannam G, Farahat LA, Youssef T, Fritzsche W, Kovács ÁT (2018) Effect of novel quercetin titanium dioxide-decorated multi-walled carbon nanotubes nanocomposite on *Bacillus subtilis* biofilm development. Materials (Basel). https://doi.org/10.3390/ma11010157

Rajith Kumar CR, Betageri VS, Nagaraju G, Pujar GH, Onkarappa HS, Latha MS (2020) One-pot green synthesis of ZnO–CuO nanocomposite and their enhanced photocatalytic and antibacterial activity. Adv Nat Sci Nanosci Nanotechnol 11:15009. https://doi.org/10.1088/2043-6254/ab6c60

Reddy DA, Lee S, Choi J, Park S, Ma R, Yang H, Kim TK (2015) Green synthesis of AgI-reduced graphene oxide nanocomposites: toward enhanced visible-light photocatalytic activity for organic dye removal. Appl Surf Sci 341:175–184. https://doi.org/10.1016/j.apsusc.2015.03.019

Reddy DHK, Lee S-M (2013) Three-dimensional porous spinel ferrite as an adsorbent for Pb(II) removal from aqueous solutions. Ind Eng Chem Res 52:15789–15800. https://doi.org/10.1021/ie303359e

Rhim J-W, Park H-M, Ha C-S (2013) Bio-nanocomposites for food packaging applications. Prog Polym Sci 38:1629–1652. https://doi.org/10.1016/j.progpolymsci.2013.05.008

Robinson T, McMullan G, Marchant R, Nigam P (2001) Remediation of dyes in textile effluent: a critical review on current treatment technologies with a proposed alternative. Bioresour Technol 77:247–255

Sabrin AAA (2015) Textile dye removal from wastewater effluents using chitosan-ZnO nanocomposite. J Text Sci Eng 05:5–8. https://doi.org/10.4172/2165-8064.1000200

Sani HA, Ahmad MB, Saleh TA (2016) Synthesis of zinc oxide/talc nanocomposite for enhanced lead adsorption from aqueous solutions. RSC Adv 6:108819–108827. https://doi.org/10.1039/C6RA24615J

Santhosh C, Kollu P, Doshi S, Sharma M, Bahadur D, VanChinathan MT, Saravanan P, Kim B-S, Grace AN (2014) Adsorption, photodegradation and antibacterial study of graphene–Fe3O4 nanocomposite for multipurpose water purification application. RSC Adv 4:28300–28308. https://doi.org/10.1039/C4RA02913E

Santhosh C, Velmurugan V, Jacob G, Jeong SK, Grace AN, Bhatnagar A (2016) Role of nanomaterials in water treatment applications: a review. Chem Eng J 306:1116–1137. https://doi.org/10.1016/j.cej.2016.08.053

Sh GAD, Zahra FA (2020) The use of titanium oxide/polyethylene glycol nanocomposite in sorption of 134 Cs and 60 Co radionuclides from aqueous solutions. J Radioanal Nucl Chem. https://doi.org/10.1007/s10967-020-07167-9

Sharma G, Bhogal S, Kumar A, Naushad M, Sharma S, Ahamad T, Stadler FJ (2020) AgO/MgO/FeO@Si_3N_4 nanocomposite with robust adsorption capacity for tetracycline antibiotic removal from aqueous system. Adv Powder Technol 31:4310–4318. https://doi.org/10.1016/j.apt.2020.09.006

Sharma G, Kumar A, Sharma S, Naushad M, Prakash Dwivedi R, Alothman ZA, Mola GT (2019) Novel development of nanoparticles to bimetallic nanoparticles and their composites: a review. J King Saud Univ Sci 31:257–269. https://doi.org/10.1016/j.jksus.2017.06.012

Sharma K, Maiti K, Kim NH, Hui D, Lee JH (2018) Green synthesis of glucose-reduced graphene oxide supported Ag-Cu_2O nanocomposites for the enhanced visible-light photocatalytic activity. Compos B Eng 138:35–44. https://doi.org/10.1016/j.compositesb.2017.11.021

Shimada T, Yasui T, Yonese A, Yanagida T, Kaji N, Kanai M, Nagashima K, Kawai T, Baba Y (2020) Mechanical rupture-based antibacterial and cell-compatible ZnO/SiO_2 nanowire structures formed by bottom-up approaches. Micromachines 11

Silva W, Rodrigues da Silva M, Takashima K (2015) Preparation and characterization of Zno/CuO semiconductor and photocatalytic activity on the decolorization of direct red 80 azodye. J Chil Chem Soc 60:2749–2751. https://doi.org/10.4067/S0717-97072015000400022

Singh V, Joung D, Zhai L, Das S, Khondaker SI, Seal S (2011) Graphene based materials: past, present and future. Prog Mater Sci 56:1178–1271. https://doi.org/10.1016/j.pmatsci.2011.03.003

Siriphannon P, Iamphaojeen Y (2018) Facile synthesis of chitosan/CuO nanocomposites for potential use as biocontrol agents. Bull Polish Acad Sci Tech Sci 66:311–316. https://doi.org/10.24425/123437

Slokar YM, Le Marechal AM (1998) Methods of decoloration of textile wastewaters. Dye Pigment 37:335–356. https://doi.org/10.1016/S0143-7208(97)00075-2

Song H, Hao L, Tian Y, Wan X, Zhang L, Lv Y (2019) Stable and water-dispersible graphene nanosheets: sustainable preparation, functionalization, and high-performance adsorbents for Pb2+. ChemPlusChem 77:379–386. https://doi.org/10.1002/cplu.201200012

Soppe AIA, Heijman SGJ, Gensburger I, Shantz A, van Halem D, Kroesbergen J, Wubbels GH, Smeets PWMH (2014) Critical parameters in the production of ceramic pot filters for household water treatment in developing countries. J Water Health 13:587–599. https://doi.org/10.2166/wh.2014.090

Sreeprasad TS, Maliyekkal SM, Lisha KP, Pradeep T (2011) Reduced graphene oxide-metal/metal oxide composites: Facile synthesis and application in water purification. J Hazard Mater 186:921–931. https://doi.org/10.1016/j.jhazmat.2010.11.100

Stan MS, Nica IC, Popa M, Chifiriuc MC, Iordache O, Dumitrescu I, Diamandescu L, Dinischiotu A (2018) Reduced graphene oxide/TiO_2 nanocomposites coating of cotton fabrics with antibacterial and self-cleaning properties. J Ind Text 49:277–293. https://doi.org/10.1177/1528083718779447

Štengl V, Bakardjieva S, Grygar TM, Bludská J, Kormunda M (2013) TiO_2-graphene oxide nanocomposite as advanced photocatalytic materials. Chem Cent J 7:1–12. https://doi.org/10.1186/1752-153X-7-41

Stoller MD, Park S, Zhu Y, An J, Ruoff RS (2008) Graphene-based ultracapacitors. Nano Lett 8:3498–3502. https://doi.org/10.1021/nl802558y

Suleman Ismail Abdalla S, Katas H, Chan JY, Ganasan P, Azmi F, Fauzi M, Busra M (2020) Antimicrobial activity of multifaceted lactoferrin or graphene oxide functionalized silver nanocomposites biosynthesized using mushroom waste and chitosan. RSC Adv 10:4969–4983. https://doi.org/10.1039/C9RA08680C

Syame SM, Mohamed WS, Mahmoud RK, Omara ST (2017) Synthesis of copper-chitosan nanocomposites and their applications in treatment of local pathogenic isolates bacteria. Orient J Chem 33:2959–2969. https://doi.org/10.13005/ojc/330632

Tayel A, Ramadan AR, El Seoud OA (2018) Titanium dioxide/graphene and titanium dioxide/graphene oxide nanocomposites: synthesis, characterization and photocatalytic applications for water decontamination. Catalysts. https://doi.org/10.3390/catal8110491

Tchobanoglous G, Burton FL, Metcalf, Eddy (1991) Wastewater engineering: treatment, disposal, and reuse

Theron J, Eugene Cloete T, de Kwaadsteniet M (2010) Current molecular and emerging nanobiotechnology approaches for the detection of microbial pathogens. Crit Rev Microbiol 36:318–339. https://doi.org/10.3109/1040841x.2010.489892

Tian Y, Wang Y, Sheng Z, Li T, Li X (2016) A colorimetric detection method of pesticide acetamiprid by fine-tuning aptamer length. Anal Biochem 513:87–92. https://doi.org/10.1016/j.ab.2016.09.004

Tripathi S, Mehrotra GK, Dutta PK (2011) Chitosan–silver oxide nanocomposite film: Preparation and antimicrobial activity. Bull Mater Sci 34:29–35. https://doi.org/10.1007/s12034-011-0032-5

Veprek S, Veprek-Heijman MJG (2008) Industrial applications of superhard nanocomposite coatings. Surf Coatings Technol 202:5063–5073. https://doi.org/10.1016/j.surfcoat.2008.05.038

Wang H, Yuan X, Wu Y, Chen X, Leng L, Wang H, Li H, Zeng G (2015) Facile synthesis of polypyrrole decorated reduced graphene oxide–Fe_3O_4 magnetic composites and its application for the Cr(VI) removal. Chem Eng J 262:597–606. https://doi.org/10.1016/j.cej.2014.10.020

Wu H, Qin M, Zhang D, Chu A, Cao Z, Jia B, Chen P, Yang S, Li X, Qu X, Volinsky AA, Menon M (2016) Synthesis and characterization of Al-doped ZnO as a prospective high adsorption material. J Am Ceram Soc 99:3074–3080. https://doi.org/10.1111/jace.14282

Yang XH, Fu HT, Wang XC, Yang JL, Jiang XC, Yu AB (2014) Synthesis of silver-titanium dioxide nanocomposites for antimicrobial applications. J Nanoparticle Res 16:2526. https://doi.org/10.1007/s11051-014-2526-8

Yang Z, Hao X, Chen S, Ma Z, Wang W, Wang C, Yue L, Sun H, Shao Q, Murugadoss V, Guo Z (2018) Long-term antibacterial stable reduced graphene oxide nanocomposites loaded with cuprous oxide nanoparticles. J Colloid Interface Sci. https://doi.org/10.1016/j.jcis.2018.08.053

Yu S, Wang X, Tan X, Wang X (2015) Sorption of radionuclides from aqueous systems onto graphene oxide-based materials: a review. Inorg Chem Front 2:593–612. https://doi.org/10.1039/C4QI00221K

Zhang K, Dwivedi V, Chi C, Wu J (2010) Graphene oxide/ferric hydroxide composites for efficient arsenate removal from drinking water. J Hazard Mater 182:162–168. https://doi.org/10.1016/j.jhazmat.2010.06.010

Zhang K, Suh JM, Lee TH, Cha JH, Choi J-W, Jang HW, Varma RS, Shokouhimehr M (2019a) Copper oxide–graphene oxide nanocomposite: efficient catalyst for hydrogenation of nitroaromatics in water. Nano Converg 6:6. https://doi.org/10.1186/s40580-019-0176-3

Zhang L, Li Y, Liu X, Zhao L, Ding Y, Povey M, Cang D (2013) The properties of ZnO nanofluids and the role of H2O2 in the disinfection activity against *Escherichia coli*. Water Res 47:4013–4021

Zhang M, Chang L, Zhao Y, Yu Z (2019b) Fabrication of zinc oxide/polypyrrole nanocomposites for brilliant green removal from aqueous phase. Arab J Sci Eng 44:111–121. https://doi.org/10.1007/s13369-018-3258-3

Zhang S, Sun D, Fu Y, Du H (2003) Recent advances of superhard nanocomposite coatings: a review. Surf Coatings Technol 167:113–119. https://doi.org/10.1016/S0257-8972(02)00903-9

Zhao G, Wen T, Chen C, Wang X (2012) Synthesis of graphene-based nanomaterials and their application in energy-related and environmental-related areas. RSC Adv 2:9286–9303

Zhao Z, Shuai W, Zhang J, Chen X (2013) Sn(IV) anions adsorption onto ferric hydroxide: a speciation-based model. Hydrometallurgy 140:135–143. https://doi.org/10.1016/j.hydromet.2013.09.010

Zhou Y, Yang J, He T, Shi H, Cheng X, Lu Y (2013) Highly stable and dispersive silver nanoparticle-graphene composites by a simple and low-energy-consuming approach and their antimicrobial activity. Small 9:3445–3454. https://doi.org/10.1002/smll.201202455

Zhu J, He J, Du X, Lu R, Huang L, Ge X (2011) A facile and flexible process of β-cyclodextrin grafted on Fe3O4 magnetic nanoparticles and host–guest inclusion studies. Appl Surf Sci 257:9056–9062. https://doi.org/10.1016/j.apsusc.2011.05.099

Zhu Y, Murali S, Cai W, Li X, Suk JW, Potts JR, Ruoff RS (2019) Graphene and graphene oxide: synthesis, properties, and applications. Adv Mater 22:3906–3924. https://doi.org/10.1002/adma.201001068

Zhu Z, Su M, Ma L, Ma L, Liu D, Wang Z (2013) Preparation of graphene oxide-silver nanoparticle nanohybrids with highly antibacterial capability. Talanta 117:449–455. https://doi.org/10.1016/j.talanta.2013.09.017

Ziashahabi A, Prato M, Dang Z, Poursalehi R, Naseri N (2019) The effect of silver oxidation on the photocatalytic activity of Ag/ZnO hybrid plasmonic/metal-oxide nanostructures under visible light and in the dark. Sci Rep 9:11839. https://doi.org/10.1038/s41598-019-48075-7

Zolfaghari G, Esmaili-Sari A, Anbia M, Younesi H, Ghasemian MB (2013) A zinc oxide-coated nanoporous carbon adsorbent for lead removal from water: optimization, equilibrium modeling, and kinetics studies. Int J Environ Sci Technol 10:325–340. https://doi.org/10.1007/s13762-012-0135-6

Zou H, Wang Y (2017) Azo dyes wastewater treatment and simultaneous electricity generation in a novel process of electrolysis cell combined with microbial fuel cell. Bioresour Technol 235:167–175. https://doi.org/10.1016/j.biortech.2017.03.093